

Linguistic Collapse: Neural Collapse in (Large) Language Models

Robert Wu

University of Toronto, Vector Institute
 rupert@cs.toronto.edu

Vardan Papyan

University of Toronto, Vector Institute
 vardan.papyan@utoronto.ca

Abstract

Neural collapse (\mathcal{NC}) is a phenomenon observed in classification tasks where top-layer representations collapse into their class means, which become equinorm, equiangular and aligned with the classifiers. These behaviours — associated with generalization and robustness — would manifest under specific conditions: models are trained towards zero loss, with noise-free labels belonging to balanced classes, which do not outnumber the model’s hidden dimension. Recent studies have explored \mathcal{NC} in the absence of one or more of these conditions to extend and capitalize on the associated benefits of ideal geometries. Language modelling presents a curious frontier, as *training by token prediction* constitutes a classification task where none of the conditions exist: the vocabulary is imbalanced and exceeds the embedding dimension; different tokens might correspond to similar contextual embeddings; and large language models (LLMs) in particular are typically only trained for a few epochs. This paper empirically investigates the impact of scaling the architectures and training of causal language models (CLMs) on their progression towards \mathcal{NC} . We find that \mathcal{NC} properties that develop with scale (and regularization) are linked to generalization. Moreover, there is evidence of some relationship between \mathcal{NC} and generalization independent of scale. Our work thereby underscores the generality of \mathcal{NC} as it extends to the novel and more challenging setting of language modelling. Downstream, we seek to inspire further research on the phenomenon to deepen our understanding of LLMs — and neural networks at large — and improve existing architectures based on \mathcal{NC} -related properties. Our code is hosted on GitHub: <https://github.com/rhubarbwu/linguistic-collapse>.

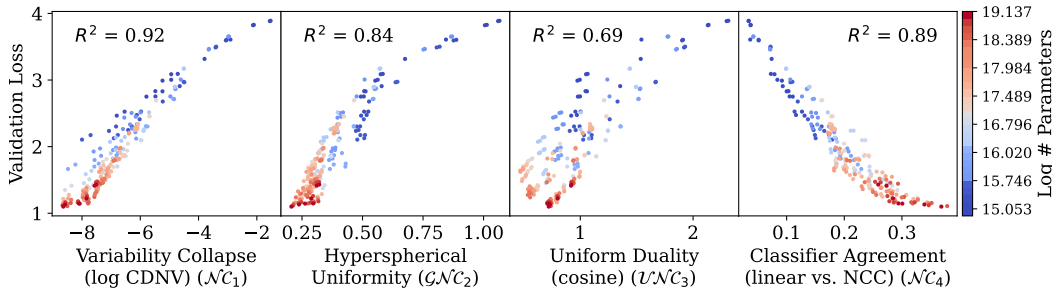


Figure 1: Simultaneous development of the four *neural collapse* (\mathcal{NC}) [1] properties in 230 causal language models trained on TinyStories [2], alongside improvement in generalization (i.e. validation performance). Left to right: \mathcal{NC}_1) within-class (representation) variability collapse; $\mathcal{GN}\mathcal{C}_2$) hyperspherical uniformity of class means; $\mathcal{UN}\mathcal{C}_3$) uniform duality between class means and corresponding classifiers; and \mathcal{NC}_4) agreement between token (maximum a prior) classifiers and implicit nearest-class centre classifiers. Coloured by model size and annotated with coefficient of determination (R^2).

1 Introduction

1.1 Neural Collapse

A learning phenomenon known as *neural collapse* (\mathcal{NC}) emerges during the terminal phase of training (TPT) deep neural networks with cross-entropy (CE) loss for classification tasks.[1] It was originally characterized as the co-occurrence of the following properties in a model’s top-layer (also known as last-layer) representations (also known as features or embeddings) and linear classifier weights:

- (\mathcal{NC}_1) **Within-class variability collapse:** Top-layer representations collapse to their class means.
- (\mathcal{NC}_2) **Convergence to a simplex ETF:** Class means tend towards equinorm and equiangular vectors when centred about the global average. The resulting geometry — known as a simplex *equiangular tight frame* (ETF) — maximizes pairwise angles and distances.
- (\mathcal{NC}_3) **Convergence to self-duality:** Linear classifier weight vectors converge to their corresponding top-layer class mean vectors, and thus also form a simplex ETF.
- (\mathcal{NC}_4) **Nearest decision rule:** Linear classifiers approximate a nearest-class centre (NCC) classifier: top-layer representations predict the class with the closest mean (implied by \mathcal{NC}_1 -3).

These behaviours, often associated with improved generalization and robustness [3–5] (among other benefits, such as those discussed in §1.4), traditionally manifest under the following conditions:

- Rq1) **Few classes:** The number of classes is upper-bounded by the embedding dimension plus one: $C \leq d + 1$; this is required to construct a perfect simplex ETF.
- Rq2) **Balanced classes:** The number of samples is equal across classes: $N_c = N_{c'}, \forall c \neq c'$.
- Rq3) **Noise-free labels:** Identical (or very similar) embeddings should belong to the same class.
- Rq4) **Sufficient training (TPT):** The model is trained past zero error, towards zero loss.

Absent these conditions, one does not typically anticipate \mathcal{NC} . Since then, follow-up studies have extended beyond and proposed techniques of quantifying or achieving \mathcal{NC} (discussed in Section 2).

1.2 (Large) Language Models

\mathcal{NC} is a phenomenon observed specifically in classification tasks. While not traditionally thought of as classifiers, language models — including large language models (LLMs) — learn to model aleatoric uncertainty, which can be viewed as stochastic token prediction [6]. For instance, masked language models (MLMs) such as BERT [7] predict one or several masked tokens within an input sequence based on the surrounding *context*. Likewise, autoregressive or causal language models (CLMs) such as GPT [8] predict the next token in a sequence given the *context* of previous tokens. Most of these models are essentially (*pre-*)trained by token classification on their vocabularies. This parallel — also drawn by [9] — raises a few natural questions:

1. Does the pre-training stage of a language model exhibit \mathcal{NC} ?
2. How do scaling and other training configurations influence \mathcal{NC} in (L)LMs?
3. To what extent is \mathcal{NC} in (L)LMs correlated with their generalization abilities?
4. Do such correlations, between \mathcal{NC} and improved generalization, persist independent of the (potential confounders of) model size and training?

To address these, we first examine the specific settings of training CLMs as they are opposed (\neg) to the traditional prerequisites (R1-4, §1.1) for \mathcal{NC} to manifest.

- \neg Rq1) **Many classes:** The unique tokens found in language modelling vocabularies are vast, usually numbering in the tens of thousands and far exceeding the hidden dimension [10].
- \neg Rq2) **Imbalanced classes:** The distribution of tokens in natural language is typically very imbalanced [11, 12], as is the case in TinyStories [2], the dataset we use (Appendix Figure 4). It has an average of 16K samples per class but a standard deviation of over 32K.

- Rq3) **Ambiguous contexts:** There may exist very similar or even identical contexts followed by different tokens in the natural language data [13]. For instance, over half of the sequences in TinyStories [2] lead with “Once upon a time”, but only three-quarters of these follow with a comma (“Once upon a time, ”). In other words, there is almost certainly some *ambiguity* to contend with in our context embeddings.
- Rq4) **Undertraining:** Most practical language models (including LLMs) are not trained for more than a few epochs [14, 15]. Further optimization typically renders diminishing returns in improving evaluation performance [16] long before any possible TPT.

1.3 Contributions

We train a suite of Transformer-based [17] CLMs¹ across a grid of model widths, depths, and training epochs on the TinyStories dataset [2] to assess the degrees to which \mathcal{NC} properties develop and how they relate to generalization performance. Our findings (summarized in Figure 1) reveal:

- **Emergence of \mathcal{NC} with scale:** As we scale model size and training, the properties of \mathcal{NC} emerge; within-class variability (\mathcal{NC}_1) and interference are reduced while hyperspherical uniformity (\mathcal{GNC}_2), uniform duality (\mathcal{UNC}_3), and classifier agreement (\mathcal{NC}_4) improve.
- **Progression towards hyperspherical uniformity:** Class means, while unable to form a simplex ETF (\mathcal{NC}_2), nonetheless tend towards uniform dispersion on a hypersphere, a geometry theorized by [18] and formalized by [19] as *hyperspherical uniformity* (\mathcal{GNC}_2).
- **Tendency towards uniform duality:** Direct alignment (self-duality) between class means and classifiers (\mathcal{NC}_3) does not appear to develop with scale. Instead, the variability of (mis)alignment across classes decreases with width and training, suggesting its minimization – which we term *uniform duality* (\mathcal{UNC}_3) – may be more cohesive with \mathcal{NC} .
- **Correlation between \mathcal{NC} and generalization:** The developments of \mathcal{NC} properties are correlated with improved validation performance. We show these correlations to persist even when fixing the (potential confounders of) model architecture and training by simply varying the random seeds for initialization and data shuffling. This suggests that \mathcal{NC} is not simply a side-effect of training, but possibly a factor of generalization in its own right.

1.4 Significance

Recently, methods building on \mathcal{NC} have found use in deep learning at large. We highlight areas such as federated learning [20], graph neural networks [21], incremental/continual learning [22–24], meta-learning [24, 25], out-of-distribution detection [26–28], privacy [29, 30], learning theory [31–36] transfer learning [3, 5, 37–40], and even LLM prompting [41]. With our results, we aim to extend insights from such contributions and other related works to the autoregressive language modelling domain and ultimately assist researchers in improving and interpreting their (L)LMs.

2 Related Works

\mathcal{NC} was initially observed in image classification tasks such as on CIFAR-10/100 [42] and ImageNet [43]. Since then, the phenomenon has been further studied both theoretically and empirically [5, 18, 35, 44–66], with several works venturing into settings without some of the traditional prerequisites (–Rq1–4, §1.2) and proposing adaptations of the analysis framework or optimization procedures:

A large number of classes (–Rq1) \mathcal{NC} established the simplex ETF as an optimal configuration. However, a perfect simplex ETF (\mathcal{NC}_2) requires that the number of classes C not exceed $d + 1$ where d is the embedding dimension. This requirement that d be sufficiently large is impractical when the classes number beyond the thousands.² For instance, GPT-2 [68] and Llama 3.1 [69] have vocabularies of around 50K and 128K tokens, respectively.

In such a scenario, one might still expect class means to be uniformly distributed on a d -dimensional hypersphere [18]. [19] formalize this as *hyperspherical uniformity* within a *generalized neural*

¹Our models range from 3.4M (small) to 205M (large), so we inclusively use “CLM” instead of “LLM”.

²Following [67], one might describe such a setting ($C > d + 1$) as a model “in superposition”.

collapse (\mathcal{GNC}) framework, which [9] then empirically demonstrate. These latter two works mention language modelling as applicable for \mathcal{GNC} ; [9] even framed token prediction as a classification task, just as we do. We remark however that both earlier works *simulate* a large number of classes by drastically shrinking the embedding dimension. In contrast, we study next-token prediction, using the full class space (vocabulary) with an imbalanced token distribution and ambiguous samples.

Class imbalance ($\neg Rq2$) \mathcal{NC} traditionally assumed that classes were sample-balanced. Since then, follow-up works have investigated the effect of class imbalance on the prevalence of \mathcal{NC} . [47] studied the *layer-peeled model* (LPM) and discovered that *minority collapse* occurs when classes are imbalanced across two equally-sized groups of classes; a threshold for minority collapse was later characterized by [35]. [52] showed that \mathcal{NC} still occurs in such an LPM when the classifier is initialized as a fixed ETF. [70] introduced *simplex-encoded-label interpolation* (SELI) but noted that more severe imbalance worsens even this geometry. Recently, feature regularization has been employed to induce \mathcal{NC} and improve generalization in class-imbalanced settings [58, 61, 62].

Multi-label classification ($\neg Rq3$) In some problems, one might encounter mixed or multi-label samples, be they natural or due to noise or augmentation [71, 72]. \mathcal{NC} was also recently studied for such data by [73], who observed that multi-label class means arrive at the average of their labels' respective means. They also devise an augmented CE loss function to accommodate such samples.

Likewise, most of our ambiguous samples could be considered multi- or soft-label: identical (or very similar) context samples with different hard token labels ($\neg Rq3$). Under popular CLM pre-training (teacher-forcing with CE loss), this effectively precludes the prospect of achieving zero classification error and potentially introduces irreducible noise.

A recent study showed that memorization of noisy labels likely leads to degradation of \mathcal{NC} [60].

Early stages of training ($\neg Rq4$) [53] studied \mathcal{NC} in small ResNet [74] models that had not yet converged (similar to most LLMs). They show that within-class variability drops and “plateaus” (\mathcal{NC}_1) earlier than other \mathcal{NC} metrics, a result that we also observe (§4.1, Figures 6, 7).

Natural language processing (NLP) An earlier study reported that the ratio of within-class to between-class covariances of word embeddings increases with model depth [75, 76], seemingly at odds with \mathcal{NC}_1 . It can, however, be distinguished from literature studying layer-wise \mathcal{NC} in that it does not centre the mean representation vectors (i.e. subtract the global mean).

[19] fine-tuned BERT [7] using their *hyperspherical uniformity gap* (HUG) objective on binary classification tasks from the GLUE benchmark [77]. [78] conducted a tangentially-related investigation of convolutional neural networks for few-class semi-supervised clustering in which they identify \mathcal{NC} . Our work is distinct from these in several ways: a) our class space far exceeds our embedding dimension ($C \gg d + 1$) because we classify on the full token vocabulary; b) we analyze embeddings at a token-level granularity rather than at the sequence level; and c) our next-token prediction is causal (context-dependent) as opposed to the per-sample independence of their few-category classification.

A more related work studied *feature collapse* in individual word representations [79], but the authors note that their analysis is limited to shallow NLP modelling on more rigid and tabular text data.

3 Methodology

Below we describe the training setup for our CLMs (§3.1), procedures³ for collecting top-layer embeddings (§3.2, 3.7), and measurements of \mathcal{NC} and generalization (§3.4, 3.5, 3.6, 3.7, 3.8).

3.1 Dataset and Language Models

TinyStories [2] is a synthetic⁴ dataset generated by GPT-3.5 and GPT-4 using around 1500 English words a child might use. Next-token prediction is performed by sampling from the token vocabulary

³Leveraging our generic \mathcal{NC} package: <https://github.com/rhubarbwu/neural-collapse>.

⁴TinyStories was developed and evaluated as a faithful emulation of large language modelling, so we chose it for experimentation to train hundreds of CLMs and analyze embeddings at a low cost. See Appendix A.

$\mathbb{V} = \llbracket 1, 29233 \rrbracket$, which for our purposes can therefore be framed as classification among $C = 29,233$ classes.⁵ Following the GPT-style preprocessing regime [8], raw sequences are packed into S chunks of size T , providing $N = S(T - 1)$ token samples for training.⁶ Details are listed in Appendix A.

We use 30 CLM architectures based on GPT Neo [80], configured similarly to [2]. They vary in width (embedding dimension) $d \in \{64, 128, 256, 512, 768, 1024\}$ and depth (number of self-attention layers) $L \in \{1, 2, 4, 8, 12\}$. Our models were trained by teacher-forcing⁷ using CE loss. For each architecture, we trained multiple models for 1, 3, and 10 epochs ablated over weight decay factors $\beta = 0.0005$ [51] and $\beta = 0.1$ [81]. Further details are listed in Appendices B, C.

3.2 Context Embeddings

Base CLMs perform next-token prediction: given a sequence of tokens $\mathbf{x}_{1:t} \in \mathbb{V}^t$, a top-layer context embedding $\mathbf{h}(\mathbf{x}_{1:t}) \in \mathbb{R}^d$ is used to predict the next token $x'_{t+1} \in \mathbb{V}$ where $1 \leq t \leq T$. A classifier for class c with weights \mathbf{w}_c and bias⁸ b_c would make maximum a prior (MAP) predictions as

$$x'_{t+1} := \operatorname{argmax}_{c \in \mathbb{V}} \langle \mathbf{w}_c, \mathbf{h}(\mathbf{x}_{1:t}) \rangle + b_c. \quad (1)$$

Class embedding means For each token class c , we are interested in the mean embedding $\boldsymbol{\mu}_c \in \mathbb{R}^d$ across sequences s and their contexts $\mathbf{x}_{1:t}^{(s)}$, where the next token $x_{t+1}^{(s)}$ is ground-truth ($t < T$) and equal to c . To centre these means, we compute their unweighted⁹ average $\bar{\boldsymbol{\mu}} \in \mathbb{R}^d$. Precisely, we take

$$\boldsymbol{\mu}_c := \frac{1}{N_c} \sum_{s=1}^S \sum_{t=1}^{T-1} \mathbf{h}\left(\mathbf{x}_{1:t}^{(s)}\right) \mathbb{I}\left(x_{t+1}^{(s)} = c\right), \quad \bar{\boldsymbol{\mu}} := \frac{1}{C} \sum_{c=1}^C \boldsymbol{\mu}_c, \quad (2)$$

where N_c is the number of samples of class c and \mathbb{I} is the (binary) indicator function.

Class embedding variances In a second pass, we accumulate the sample variance norms:¹⁰

$$\sigma_c^2 := \frac{1}{N_c} \sum_{s=1}^S \sum_{t=1}^{T-1} \left\| \mathbf{h}\left(\mathbf{x}_{1:t}^{(s)}\right) - \boldsymbol{\mu}_c \right\|_2^2 \mathbb{I}\left(x_{t+1}^{(s)} = c\right). \quad (3)$$

3.3 Homogeneity and Variability

For some collapse measures (such as $(\mathcal{G})\mathcal{NC}_2$ and \mathcal{NC}_3), we are primarily interested in the *variation* rather than the average of pairwise relationships. To that end, we also include in our analysis the *coefficient of variation* (CoV) of several measurements, which is the ratio of their standard deviations to their means: $\sigma(\cdot)/\mu(\cdot)$. We can interpret this as a normalized measure of variability.

3.4 Signal-to-Noise Ratio — $\mathcal{NC}1$

The ability to disambiguate between classes depends on the ratio of within-class to between-class variabilities. Building upon foundational works [85, 86], \mathcal{NC} originally measured variability through an inverse *signal-to-no ratio* (SNR), whose minimization constitutes *within-class variability collapse* (\mathcal{NC}_1). We instead employ a *class-distance normalized variance* (CDNV) similar to [3]:

$$\hat{\sigma}_{c,c'} := \frac{1}{\|\boldsymbol{\mu}_c - \boldsymbol{\mu}_{c'}\|_2^k} \cdot \frac{\sigma_c^2 + \sigma_{c'}^2}{2\|\boldsymbol{\mu}_c - \boldsymbol{\mu}_{c'}\|_2^2}, \quad \forall c \neq c'. \quad (4)$$

Our metric differs in that we divide by an additional power $\|\boldsymbol{\mu}_c - \boldsymbol{\mu}_{c'}\|_2^k$ of the mean distance norm. This further downweights the CNDV within well-separated class pairs in favour of emphasizing more

⁵Although the GPT-Neo [80] tokenizer has over 50K tokens, only a subset vocabulary appears in TinyStories.

⁶We cannot use the first ground-truth nor the last predicted token in any chunk.

⁷Parallelized training using sequences' ground-truth labels for context as opposed to predicted tokens.

⁸Similar to many causal LLMs [80–84], our classifiers do not include additive biases, so $b_c = 0$.

⁹Different from most literature where classes were balanced and weighting is already equal.

¹⁰This sample variance is computed across all unnormalized dimensional entries.

mutually noisy pairs. We found this augmented CDNV with $k = 2$ to be especially useful in our setting of many imbalanced and variably confusable token classes.

These pairwise measures constitute the off-diagonal¹¹ entries of a symmetric matrix in $\mathbb{R}^{C \times C}$, whose average we use as an inverse SNR. Within-class variability collapse is then re-characterized by the minimization of this quantity: $\hat{\sigma}_{c,c'} \rightarrow 0, \forall c \neq c'$. This alternative convergence is empirically faithful to \mathcal{NC}_1 but more robust and numerically stable [3].

3.5 Geometric Structures — $(\mathcal{G})\mathcal{NC}_2$

The separability of our representations also depends on the geometric structures found in our embeddings. [1] characterize \mathcal{NC}_2 as convergence to a *simplex equiangular tight frame* (ETF) [87, 88].

Equinormness Such a near-orthonormal configuration firstly implies that class means are equinorm:

$$\log \|\boldsymbol{\mu}_c - \bar{\boldsymbol{\mu}}\|_2 - \log \|\boldsymbol{\mu}_{c'} - \bar{\boldsymbol{\mu}}\|_2 \rightarrow 0, \quad \forall c \neq c'. \quad (5)$$

We measure CoV in the *logarithms* of class mean norms to assess “equinormness”.

Equiangularity \mathcal{NC}_2 also entails that class means are equiangular about their centre $\bar{\boldsymbol{\mu}}$: pairwise distances and angles between their class means should be maximized and similar. Following [1], we measure *interference* (sometimes known as similarity or *coherence* [89, 90]). Its minimization,

$$\left\langle \frac{\boldsymbol{\mu}_c - \bar{\boldsymbol{\mu}}}{\|\boldsymbol{\mu}_c - \bar{\boldsymbol{\mu}}\|_2}, \frac{\boldsymbol{\mu}_{c'} - \bar{\boldsymbol{\mu}}}{\|\boldsymbol{\mu}_{c'} - \bar{\boldsymbol{\mu}}\|_2} \right\rangle \rightarrow \frac{-1}{C-1}, \quad \forall c \neq c', \quad (6)$$

together with equinormness (Equation 5) constitute convergence to a simplex ETF. Although this geometry is not ultimately attainable since there are too many classes ($C > d + 1$), it can still be meaningful to measure a model’s tendency towards one. As with CDNV noise (Equation 4), pairwise interferences form off-diagonal¹² entries in a symmetric matrix in $\mathbb{R}^{C \times C}$. The minimization of CoV in interferences therefore expresses the degree of “equiangularity”.

Hyperspherical uniformity A relaxation from the ETF is *hyperspherical uniformity* ($(\mathcal{G}\mathcal{NC}_2)$), with mean vectors $\boldsymbol{\mu}_c$ uniformly distributed on the d -dimensional hypersphere [18, 19]. We gauge the degree of this uniformity with pairwise interactions under a logarithmic inverse distance kernel:¹³

$$\log \left\| \frac{\boldsymbol{\mu}_c - \bar{\boldsymbol{\mu}}}{\|\boldsymbol{\mu}_c - \bar{\boldsymbol{\mu}}\|_2} - \frac{\boldsymbol{\mu}_{c'} - \bar{\boldsymbol{\mu}}}{\|\boldsymbol{\mu}_{c'} - \bar{\boldsymbol{\mu}}\|_2} \right\|^{-1}, \quad \forall c \neq c'. \quad (7)$$

3.6 Alignment Between Classifiers and Class Mean Embeddings — $(\mathcal{U})\mathcal{NC}_3$

The linear classifiers $\{\mathbf{w}_c\}_{c=1}^C$ lie in a dual vector space to that of the class means $\{\boldsymbol{\mu}_c\}_{c=1}^C$. While convergence to self-duality (\mathcal{NC}_3) was initially measured as distances [1] between class means and classifiers (Equation 11), we follow [5] to inspect class-wise cosine similarities:¹⁴

$$\left\langle \frac{\mathbf{w}_c}{\|\mathbf{w}_c\|_2}, \frac{\boldsymbol{\mu}_{c'} - \bar{\boldsymbol{\mu}}}{\|\boldsymbol{\mu}_{c'} - \bar{\boldsymbol{\mu}}\|_2} \right\rangle \rightarrow 1, \quad \forall c \in \mathbb{V}. \quad (8)$$

For intuition analogous to that for equinormness and equiangularity (§3.5), we also measure *uniform duality* (\mathcal{UNC}_3) as the minimization of the CoV of these similarities (Appendices N, O).

3.7 Agreement of the Classifiers — \mathcal{NC}_4

Finally, \mathcal{NC}_4 is described as the simplification of the linear classifier’s MAP predictions (Equation 1) for *test*¹⁵ points to those of the implicit *nearest-class centre* (NCC) classifier:

$$\operatorname{argmax}_{c \in \mathbb{V}} \langle \mathbf{w}_c, \mathbf{h} \rangle + b_c \rightarrow \operatorname{argmin}_{c \in \mathbb{V}} \|\mathbf{h} - \boldsymbol{\mu}_c\|_2. \quad (9)$$

¹¹The main diagonal of CDNVs is undefined (due to the zero denominator) and ignored.

¹²The main diagonal of interferences is equal to 1 (maximal coherence or self-similarity).

¹³Following [19], we employ the logarithmic inverse distance kernel $K_{\log}(\mathbf{a}, \mathbf{b}) = \log \|\mathbf{a} - \mathbf{b}\|_2^{-1}$ for its ability to emphasize gaps between small distances while scaling down the effect of larger distances.

¹⁴Dot-product would be confounded by norms and therefore inappropriate for similarity up to rescaling.

¹⁵We used the validation set since it was not used for training or hyperparameter optimization.

We calculate¹⁶ agreement as the proportion of samples on which the classifiers agree:¹⁷

$$\frac{1}{N_{\text{val}}} \sum_{s=1}^{S_{\text{val}}} \sum_{t=1}^{T_{\text{val}}-1} \mathbb{I} \left(x'_{t+1}^{(s)} = \operatorname{argmin}_{c \in \mathcal{V}} \left\| \mathbf{h} \left(x_{1:t}^{(s)} \right) - \boldsymbol{\mu}_c \right\|_2 \right). \quad (10)$$

3.8 Probing a Relationship Between \mathcal{NC} and Generalization

To isolate the effect of \mathcal{NC} on generalization independent of model scaling and training (if it exists), we selected a two-layer 768-wide architecture of which to train twenty more instances with weight decay $\beta = 0.0005$, each with a different data shuffling seed. We then followed the remainder of the pipeline described above to collect and analyze embeddings with respect to \mathcal{NC} . Finally, we performed a permutation test with 10^4 trials to determine the statistical significance of any correlation between \mathcal{NC} and generalization that remains when we hold constant all factors but shuffling seeds.

4 Experimental Results

In this section, we present the results from our empirical study on scaling and generalization:

- (\mathcal{NC}_1) Within-class variability is reduced across model scale (more so by width than depth) and training (up to 6 epochs), and is tightly correlated with validation performance.
- (\mathcal{NC}_2) Equinormness/equiangularity shows some improvement with scale, training, and performance. Hyperspherical uniformity (\mathcal{GNC}_2) also improves but more clearly and consistently.
- (\mathcal{NC}_3) Our models fail to achieve self-duality: class means do not align with classifiers. However, uniform duality (\mathcal{UNC}_3) is correlated with model width, training, and performance.
- (\mathcal{NC}_4) Larger or more trained models exhibit closer agreement between their linear and implicit NCC classifiers. Agreement is also associated with validation performance.

4.1 Within-Class Variability Collapse — \mathcal{NC}_1

Scaling our models dramatically reduces normalized variance, which is further aided by more training epochs and stronger weight decay (Appendix Figs. 6, 7). These noise reductions tightly associate with generalization (Fig. 1, left, “ \mathcal{NC}_1 ”). The relationship is most apparent at scale.

4.2 Geometric Structures — $(\mathcal{G})\mathcal{NC}_2$

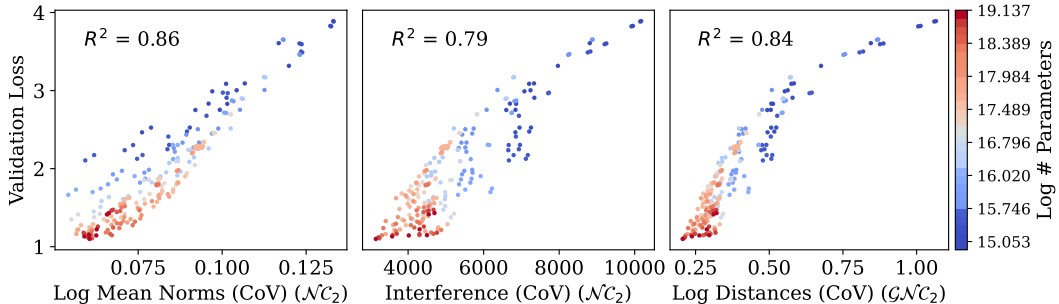


Figure 2: Validation loss is correlated with all three measurements: **(left)** equinormness (\mathcal{NC}_2) expressed as variation in logarithmic norms; **(centre)** equiangularity (\mathcal{NC}_2) as variation in interference; **(right)** hyperspherical uniformity (\mathcal{GNC}_2) as variation in logarithmic pairwise distances.

Equinormness Logarithmic class mean norms grow with model width and training (Appendix Fig. 8), and subtly with depth (Appendix Fig. 9). Meanwhile, the variation of these (logarithmic) norms consistently decreases (improving equinormness) with scale (Appendix Figs. 10, 11). Both trends correlate with improved generalization (Appendix Fig. 20).

¹⁶In practice, we use an equivalent decomposition (Eq. 12).

¹⁷Note that agreement is not equivalent to accuracy.

Equiangularity Scaling model dimensions reduces average interference (Appendix Figs. 12, 13) down to an empirical plateau of approximately 10^{-3} , which is more apparent in less-trained models. However, the variation of interference rises and persists when scaling (Appendix Figs. 14, 15), suggesting that interference becomes more concentrated between some pairs of classes. These results could be due to various factors, including but not limited to unfriendly conditions of language modelling (§1.2) or the impossibility of a perfect simplex ETF (§3.5).

Appendix Figure 21 shows only a rough performance correlation with average interference (i.e. coherence) and a more definite — albeit still noisy — one with the variation of interference (i.e. equiangularity). In other words, the limited trends we observed toward a simplex ETF suggest that the association of $\mathcal{NC}2$ with generalization begins to break down when $C > d + 1$.

Hyperspherical uniformity Logarithmic distances drop more gradually and consistently with scale (Appendix Figs. 16, 17), implying this quantity is more robust or may not face the same geometric barriers seen in conventional interference (Appendix Figs. 14, 15). Variation of these logarithmic distances is also consistently reduced with scale (Appendix Fig. 18, 19).

And finally, generalization has much stronger correlations with logarithmic distances than it has with regular interference (Fig. 2), validating the applicability of \mathcal{GNC} [19] when $C > d + 1$.

4.3 Classifier (Mis)alignment and Duality — $(\mathcal{U})\mathcal{NC}3$

Model width (d) is correlated faintly with the average similarity between class means and their respective classifiers (Appendix Fig. 23), but strongly with variation in similarity (Appendix Fig. 25). The relationships to generalization follow the same pattern (Fig. 3), suggesting that uniform duality (\mathcal{UNC}_3) might serve as a better \mathcal{NC} property than self-duality (\mathcal{NC}_3) overall; we discuss this in §5.1.

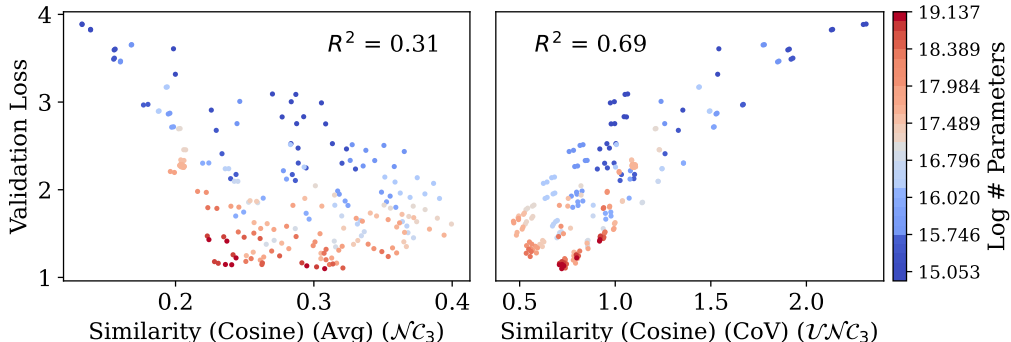


Figure 3: Validation loss shows a negligible relationship with self-duality (\mathcal{NC}_3 , left) and some correlation with uniform duality (\mathcal{UNC}_3 , right). In other words, \mathcal{UNC}_3 develops with scale and correlates with generalization much better than \mathcal{NC}_3 .

4.4 Classifier Agreement — $\mathcal{NC}4$

The linear and NCC classifiers agree on far more examples than random chance, and model scaling encourages this agreement (Appendix Figs. 29, 30). Increasing width for certain depths happens to plateau or even regress the agreement rate, but this limitation is overcome with further training. And finally, agreement is a strong indicator of generalization (Fig. 1, right, \mathcal{NC}_4).

5 Analysis

We find that \mathcal{NC} is generally promoted by model size and training and correlated with generalization (validation performance). We also discern some of this correlation independent of scale (§5.1).

Table 1: Permutation test of \mathcal{NC} measurements with respect to validation loss. Twenty-one (21) identical two-layer 768-wide models were trained with different data shuffling seeds and permuted with 10^4 trials. The p -values below 0.05 (bolded) show those properties to be statistically significant.

Property	Measurement	R^2 Correlation (\uparrow)	p -value (\downarrow)
\mathcal{NC}_1	Within-Class Variability Collapse	0.192011	0.0485
\mathcal{NC}_2	Equinormness	0.026174	0.4870
\mathcal{NC}_2	Equiangularity	0.218574	0.0317
\mathcal{GNC}_2	Hyperspherical Uniformity	0.487935	0.0002
\mathcal{NC}_3	Self-Duality	0.322210	0.0063
\mathcal{UNC}_3	Uniform Duality	0.000036	0.9784
\mathcal{NC}_4	Classifier Agreement	0.490278	0.0001

5.1 Neural Collapse’s Relationship with Generalization

Table 1 presents the correlation scores of \mathcal{NC} metrics with generalization alongside their associated p -values from the permutation tests described in §3.8. The majority of the correlations are statistically significant ($p < 0.05$) independent of scale, affirming that \mathcal{NC} is correlated with generalization.

5.2 Duality of Duality

The dichotomy of self-duality (\mathcal{NC}_3) and uniform duality (\mathcal{UNC}_3) is rather conspicuous. Our main experiments find that \mathcal{NC}_3 does not consistently develop with scale while \mathcal{UNC}_3 does (Fig. 3). However, within a fixed scale, the opposite is true, implying that \mathcal{UNC}_3 may be confounded by model capacity while \mathcal{NC}_3 is a subtle and fine-grained indicator of generalization.

5.3 The Effect of Weight Regularization

Our models trained with either weight decay factor exhibited very similar patterns in the emergence of \mathcal{NC} (or lack thereof), but the more aggressive factor $\beta = 0.1$ resulted in stronger development of \mathcal{NC} properties than with $\beta = 0.0005$ (Appendices E, F, G, H, I, J, K, M, N, P). These findings empirically affirm $\beta = 0.1$ weight decay as sensible for CLM pre-training [81], and concur with [51] on the pivotal role that appropriate regularization plays in the emergence of \mathcal{NC} .

6 Limitations

Neural collapse While to the best of our knowledge, no previous work has studied realistic stochastic token prediction, it is possible that the quantities that we measure are not perfectly suited for \mathcal{NC} in language modelling. As we described in §1.1, the \mathcal{NC} framework does not translate neatly to the language modelling space due to many adverse conditions, so full convergence to \mathcal{NC} in the TPT was highly improbable. This paper leaves much room for future work to better adapt \mathcal{NC} for next-token prediction, which we discuss further in Section 7.

Language modelling Our work focused on autoregressive pre-training in its most basic form. We did not conduct experiments into encoder, multi-modal, or instruction-tuned models. Post-training techniques such as supervised fine-tuning, reinforcement learning with human feedback [91] or direct preference optimization [92] are also out-of-scope. This paper uses validation CE loss as the sole indicator of performance, leaving out any downstream task evaluations.

Confounder of model scale The models that we used in our permutation test (§5.1, Table 1) are only of a single small architecture trained for one epoch with relatively weak weight regularization ($\beta = 0.0005$). Therefore, our experimental results on scale-independent links between \mathcal{NC} and generalization may not necessarily translate to larger models. Further investigation on (foundation) LLMs orders of magnitude larger than our CLMs trained with modern NLP methods would provide more robust insight into any direct correlations.

7 Discussion

Layer/depth-wise neural collapse Past works have established that properties resembling \mathcal{NC} evolve as a function of model depth [4, 36, 53, 56, 59, 60, 93–104]. Layer-wise \mathcal{NC} — sometimes dubbed *deep neural collapse* (DNC) [53, 59] — and related phenomena at intermediate layers remain an interesting subtopic. We leave their study and induction in CLMs (like [105]) as future work.

Learning to collapse Given the evidence for the development of \mathcal{NC} and associated generalization under various loss functions [19, 49, 60, 100, 106–108] in other domains, NLP researchers may still benefit from analyzing, adapting or training towards \mathcal{NC} . As alluded to earlier, the simplex ETF and even the CE loss may not be truly optimal for this problem setting, so we anticipate future works to both construct more amenable geometries with better-suited objectives and then capitalize on their benefits downstream. As discussed in §2, there is an abundance of literature in \mathcal{NC} , some of which could potentially adapt \mathcal{NC} to be useful for NLP; we hope to inspire more such investigations.

LLM Evaluations Researchers in NLP and multimodal settings are ultimately interested in measuring model performance on practical tasks; notable benchmarks include GLUE [77], MMLU [109], and BIG-bench [110]. However, several contemporaries [111–113] have demonstrated that models’ downstream capabilities are roughly correlated with their abilities to effectively compress their pre-training data. Based on their findings, our application of the \mathcal{NC} framework to the pre-training stage of CLMs against validation CE loss should be an appropriate first step in this intersection. Looking forward, we anticipate exciting analysis for language modelling tasks or benchmarks, especially on creativity and retrieval for natural language understanding and generation.

Conversely, some form of \mathcal{NC} could be an alternative evaluation. Although it would be prohibitively expensive to measure \mathcal{NC} on the vast and sometimes obscure pre-training data of most frontier production LLMs, doing so on a small set of in-distribution data (i.e. test set) would be realistic.

Interpretability At a high level, the number and density of clusters for a token can reflect its learned meanings and uses. This would be particularly useful as LLMs adapt to ever-evolving language and further expansion into non-English domains. Our formulae (Section 3) and results (Section 4) expose the pairwise token class interactions in noise, interference, classifier duality, and classifier agreement in the top-level features. Similarly to works in other domains [21, 55, 72, 114], these \mathcal{NC} metrics can serve as a form of low-level interpretability to aid understanding certain behaviours of (L)LMs. Between tokens, one can often discern how related or interchangeable words are based on their pair-wise interactions, or how antithetical or unrelated they are based on orthogonality. For example, we present a rudimentary analysis of homonyms and English first names in Appendix Q.

Fairness Foundation models are ubiquitous for their comprehensive capabilities and adaptability. As previous work discussed class imbalance [35, 58, 61, 62], our work may extend these strategies to measure and perhaps promote fairness in foundation LLMs, some of which are designed to be multilingual or multicultural. For example, [115] contemporarily explores the use of $\mathcal{UNC}3$ to mitigate biases in BERT-based [7] models.

While \mathcal{NC} itself would not lead to unfairness, its potential interpretability may, in theory, enable an (adversarial) agent to measure and optimize for (un)fairness as they manipulate an LLM.

8 Conclusion

In this paper, we apply the *neural collapse* (\mathcal{NC}) framework to the next-token prediction problem, where models are undertrained and next-tokens are variably drawn from numerous and imbalanced token classes. We leverage canonical and more recent metrics to demonstrate that \mathcal{NC} emerges as we scale the size and training of hundreds of causal language models. Our results show a correlation between \mathcal{NC} and generalization, a relationship that persists even when the model scale is fixed.

In the short term, our work presents rudimentary techniques to analyze and interpret token-level properties of (L)LMs. We anticipate future work to suitably adapt \mathcal{NC} (and related frameworks) to the still-fresh frontier of autoregressive language modelling. Researchers could then effectively capitalize on previous learnings from \mathcal{NC} to better understand and improve the pre/post-training processes of increasingly complex and large language (multimodal) models.

Acknowledgements

We thank Elliot Creager, David Glukhov, Daniel Johnson, Jivan Waber, and Colin Raffel for their helpful feedback and stimulating discussions. Aditya Mehrotra and Yu Bo Gao provided technical assistance in our implementations. We acknowledge the support of the Natural Sciences and Engineering Research Council (NSERC) of Canada (www.nserc-crsng.gc.ca/). This research was enabled in part by resources from Calcul Québec (www.calculquebec.ca), the Digital Research Alliance of Canada (www.alliancecan.ca), and the Vector Institute (www.vectorinstitute.ai).

References

- [1] Vardan Petyan, X. Y. Han, and David L. Donoho. Prevalence of neural collapse during the terminal phase of deep learning training. *Proceedings of the National Academy of Sciences*, 117(40):24652–24663, sep 2020. doi: 10.1073/pnas.2015509117. URL <https://www.pnas.org/doi/full/10.1073/pnas.2015509117>.
- [2] Ronen Eldan and Yuanzhi Li. Tinystories: How small can language models be and still speak coherent english?, 2023. URL <https://arxiv.org/abs/2305.07759>.
- [3] Tomer Galanti, András György, and Marcus Hutter. On the role of neural collapse in transfer learning, 2022. URL <https://arxiv.org/abs/2112.15121v2>.
- [4] Tomer Galanti, Liane Galanti, and Ido Ben-Shaul. On the implicit bias towards minimal depth of deep neural networks, 2022. URL <https://arxiv.org/abs/2202.09028v9>.
- [5] Vignesh Kothapalli. Neural collapse: A review on modelling principles and generalization. *Transactions on Machine Learning Research*, 2023. ISSN 2835-8856. URL <https://openreview.net/forum?id=QTXocpAP9p>.
- [6] Emily M. Bender, Timnit Gebru, Angelina McMillan-Major, and Shmargaret Shmitchell. On the dangers of stochastic parrots: Can language models be too big? In *Proceedings of the 2021 ACM Conference on Fairness, Accountability, and Transparency*, FAccT ’21, page 610–623, New York, NY, USA, 2021. Association for Computing Machinery. ISBN 9781450383097. doi: 10.1145/3442188.3445922. URL <https://doi.org/10.1145/3442188.3445922>.
- [7] Jacob Devlin, Ming-Wei Chang, Kenton Lee, and Kristina Toutanova. Bert: Pre-training of deep bidirectional transformers for language understanding, 2019. URL <https://arxiv.org/abs/1810.04805>.
- [8] Alec Radford, Karthik Narasimhan, Tim Salimans, Ilya Sutskever, et al. Improving language understanding by generative pre-training. 2018.
- [9] Jiachen Jiang, Jinxin Zhou, Peng Wang, Qing Qu, Dustin Mixon, Chong You, and Zihui Zhu. Generalized neural collapse for a large number of classes, 2023. URL <https://arxiv.org/abs/2310.05351>.
- [10] Zhilin Yang, Zihang Dai, Ruslan Salakhutdinov, and William W. Cohen. Breaking the softmax bottleneck: A high-rank rnn language model, 2018. URL <https://arxiv.org/abs/1711.03953>.
- [11] C. E. Shannon. A mathematical theory of communication. *The Bell System Technical Journal*, 27(3):379–423, 1948. doi: 10.1002/j.1538-7305.1948.tb01338.x.
- [12] P Sargent Florence. Human behaviour and the principle of least effort. *The Economic Journal*, 60(240):808–810, 1950.
- [13] Daniel Jurafsky and James H Martin. Speech and language processing: An introduction to natural language processing, computational linguistics, and speech recognition, 2009.
- [14] Jared Kaplan, Sam McCandlish, Tom Henighan, Tom B. Brown, Benjamin Chess, Rewon Child, Scott Gray, Alec Radford, Jeffrey Wu, and Dario Amodei. Scaling laws for neural language models, 2020. URL <https://arxiv.org/abs/2001.08361v1>.

- [15] Jordan Hoffmann, Sebastian Borgeaud, Arthur Mensch, Elena Buchatskaya, Trevor Cai, Eliza Rutherford, Diego de Las Casas, Lisa Anne Hendricks, Johannes Welbl, Aidan Clark, Tom Hennigan, Eric Noland, Katie Millican, George van den Driessche, Bogdan Damoc, Aurelia Guy, Simon Osindero, Karen Simonyan, Erich Elsen, Jack W. Rae, Oriol Vinyals, and Laurent Sifre. Training compute-optimal large language models, 2022. URL <https://arxiv.org/abs/2203.15556v1>.
- [16] Niklas Muennighoff, Alexander M. Rush, Boaz Barak, Teven Le Scao, Aleksandra Piktus, Nouamane Tazi, Sampo Pyysalo, Thomas Wolf, and Colin Raffel. Scaling data-constrained language models, 2023. URL <https://arxiv.org/abs/2305.16264v4>.
- [17] Ashish Vaswani, Noam Shazeer, Niki Parmar, Jakob Uszkoreit, Llion Jones, Aidan N Gomez, Łukasz Kaiser, and Illia Polosukhin. Attention is all you need. *Advances in neural information processing systems*, 30, 2017.
- [18] Jianfeng Lu and Stefan Steinerberger. Neural collapse with cross-entropy loss, 2021. URL <https://arxiv.org/abs/2012.08465v2>.
- [19] Weiyang Liu, Longhui Yu, Adrian Weller, and Bernhard Schölkopf. Generalizing and decoupling neural collapse via hyperspherical uniformity gap, 2023. URL <https://arxiv.org/abs/2303.06484v2>.
- [20] Zexi Li, Xinyi Shang, Rui He, Tao Lin, and Chao Wu. No fear of classifier biases: Neural collapse inspired federated learning with synthetic and fixed classifier. In *Proceedings of the IEEE/CVF International Conference on Computer Vision*, pages 5319–5329, 2023.
- [21] Vignesh Kothapalli, Tom Tirer, and Joan Bruna. A neural collapse perspective on feature evolution in graph neural networks. *Advances in Neural Information Processing Systems*, 36, 2024.
- [22] Yibo Yang, Haobo Yuan, Xiangtai Li, Jianlong Wu, Lefei Zhang, Zhouchen Lin, Philip Torr, Dacheng Tao, and Bernard Ghanem. Neural collapse terminus: A unified solution for class incremental learning and its variants, 2023. URL <https://arxiv.org/abs/2308.01746v1>.
- [23] Qinhao Zhou, Xiang Xiang, and Jing Ma. Hierarchical task-incremental learning with feature-space initialization inspired by neural collapse. *Neural Processing Letters*, 55(8):10811–10827, 2023.
- [24] Hang Ran, Weijun Li, Lusi Li, Songsong Tian, Xin Ning, and Prayag Tiwari. Learning optimal inter-class margin adaptively for few-shot class-incremental learning via neural collapse-based meta-learning. *Information Processing & Management*, 61(3):103664, 2024. ISSN 0306-4573. doi: <https://doi.org/10.1016/j.ipm.2024.103664>. URL <https://www.sciencedirect.com/science/article/pii/S0306457324000244>.
- [25] Saaketh Medepalli and Naren Doraiswamy. On the role of neural collapse in meta learning models for few-shot learning, 2023. URL <https://arxiv.org/abs/2310.00451v2>.
- [26] Jarrod Haas, William Yolland, and Bernhard Rabus. Linking neural collapse and l2 normalization with improved out-of-distribution detection in deep neural networks, 2023. URL <https://arxiv.org/abs/2209.08378v3>.
- [27] Mouïn Ben Ammar, Nacim Belkhir, Sebastian Popescu, Antoine Manzanera, and Gianni Franchi. Neco: Neural collapse based out-of-distribution detection, 2024. URL <https://arxiv.org/abs/2310.06823>.
- [28] Jiawei Zhang, Yufan Chen, Cheng Jin, Lei Zhu, and Yuantao Gu. Epa: Neural collapse inspired robust out-of-distribution detector, 2024. URL <https://arxiv.org/abs/2401.01710v1>.
- [29] Donghao Li, Yang Cao, and Yuan Yao. Neuromixgdp: A neural collapse-inspired random mixup for private data release. In *Conference on Parsimony and Learning*, pages 480–514. PMLR, 2024.

- [30] Chendi Wang, Yuqing Zhu, Weijie J. Su, and Yu-Xiang Wang. Neural collapse meets differential privacy: Curious behaviors of noisygd with near-perfect representation learning, 2024. URL <https://arxiv.org/abs/2405.08920v2>.
- [31] Tolga Ergen, Arda Sahiner, Batu Ozturkler, John Pauly, Morteza Mardani, and Mert Pilanci. Demystifying batch normalization in relu networks: Equivalent convex optimization models and implicit regularization, 2022. URL <https://arxiv.org/abs/2103.01499v3>.
- [32] Tolga Ergen and Mert Pilanci. Revealing the structure of deep neural networks via convex duality. In Marina Meila and Tong Zhang, editors, *Proceedings of the 38th International Conference on Machine Learning*, volume 139 of *Proceedings of Machine Learning Research*, pages 3004–3014. PMLR, 18–24 Jul 2021. URL <https://proceedings.mlr.press/v139/ergen21b.html>.
- [33] Mariia Seleznova, Dana Weitzner, Raja Giryes, Gitta Kutyniok, and Hung-Hsu Chou. Neural (tangent kernel) collapse. In A. Oh, T. Naumann, A. Globerson, K. Saenko, M. Hardt, and S. Levine, editors, *Advances in Neural Information Processing Systems*, volume 36, pages 16240–16270. Curran Associates, Inc., 2023. URL https://proceedings.neurips.cc/paper_files/paper/2023/file/3477ca0ce484aa2fa42c1361ab601c25-Paper-Conference.pdf.
- [34] Matus Telgarsky. Feature selection with gradient descent on two-layer networks in low-rotation regimes, 2022. URL <https://arxiv.org/abs/2208.02789v1>.
- [35] Wanli Hong and Shuyang Ling. Neural collapse for unconstrained feature model under cross-entropy loss with imbalanced data, 2023. URL <https://arxiv.org/abs/2309.09725v2>.
- [36] Gerard Ben Arous, Reza Gheissari, Jiaoyang Huang, and Aukosh Jagannath. High-dimensional sgd aligns with emerging outlier eigenspaces, 2023. URL <https://arxiv.org/abs/2310.03010v1>.
- [37] Like Hui, Mikhail Belkin, and Preetum Nakkiran. Limitations of neural collapse for understanding generalization in deep learning, 2022. URL <https://arxiv.org/abs/2202.08384v1>.
- [38] Tomer Galanti, András György, and Marcus Hutter. Improved generalization bounds for transfer learning via neural collapse. In *First Workshop on Pre-training: Perspectives, Pitfalls, and Paths Forward at ICML 2022*, 2022. URL https://openreview.net/forum?id=VrK7pKwOhT_.
- [39] Zijian Wang, Yadan Luo, Liang Zheng, Zi Huang, and Mahsa Baktashmotagh. How far pre-trained models are from neural collapse on the target dataset informs their transferability. In *Proceedings of the IEEE/CVF International Conference on Computer Vision*, pages 5549–5558, 2023.
- [40] Xiao Li, Sheng Liu, Jinxin Zhou, Xinyu Lu, Carlos Fernandez-Granda, Zhihui Zhu, and Qing Qu. Understanding and improving transfer learning of deep models via neural collapse. *Transactions on Machine Learning Research*, 2024. ISSN 2835-8856. URL <https://openreview.net/forum?id=o8r84MzTQB>.
- [41] Didi Zhu, Zexi Li, Min Zhang, Junkun Yuan, Yunfeng Shao, Jiashuo Liu, Kun Kuang, Yinchuan Li, and Chao Wu. Understanding prompt tuning for v-l models through the lens of neural collapse, 2023. URL <https://arxiv.org/abs/2306.15955v3>.
- [42] Alex Krizhevsky and Geoffrey Hinton. Learning multiple layers of features from tiny images. Technical Report 0, University of Toronto, Toronto, Ontario, 2009. URL <https://www.cs.toronto.edu/~kriz/learning-features-2009-TR.pdf>.
- [43] Jia Deng, Wei Dong, Richard Socher, Li-Jia Li, Kai Li, and Li Fei-Fei. Imagenet: A large-scale hierarchical image database. In *2009 IEEE conference on computer vision and pattern recognition*, pages 248–255. Ieee, 2009.
- [44] Dustin G. Mixon, Hans Parshall, and Jianzong Pi. Neural collapse with unconstrained features, 2020. URL <https://arxiv.org/abs/2011.11619v1>.

- [45] Tomaso Poggio and Qianli Liao. Explicit regularization and implicit bias in deep network classifiers trained with the square loss, 2020. URL <https://arxiv.org/abs/2101.00072v1>.
- [46] Weinan E and Stephan Wojtowytscz. On the emergence of simplex symmetry in the final and penultimate layers of neural network classifiers, 2021. URL <https://arxiv.org/abs/2012.05420v3>.
- [47] Cong Fang, Hangfeng He, Qi Long, and Weijie J Su. Exploring deep neural networks via layer-peeled model: Minority collapse in imbalanced training. *Proceedings of the National Academy of Sciences*, 118(43):e2103091118, 2021.
- [48] Zhihui Zhu, Tianyu Ding, Jinxin Zhou, Xiao Li, Chong You, Jeremias Sulam, and Qing Qu. A geometric analysis of neural collapse with unconstrained features, 2021. URL <https://arxiv.org/abs/2105.02375v1>.
- [49] X.Y. Han, Vardan Papyan, and David L. Donoho. Neural collapse under MSE loss: Proximity to and dynamics on the central path. In *International Conference on Learning Representations*, 2022. URL https://openreview.net/forum?id=w1UbdvWH_R3.
- [50] Can Yaras, Peng Wang, Zhihui Zhu, Laura Balzano, and Qing Qu. Neural collapse with normalized features: A geometric analysis over the riemannian manifold. *Advances in neural information processing systems*, 35:11547–11560, 2022.
- [51] Akshay Rangamani and Andrzej Banburski-Fahey. Neural collapse in deep homogeneous classifiers and the role of weight decay. In *ICASSP 2022 - 2022 IEEE International Conference on Acoustics, Speech and Signal Processing (ICASSP)*, pages 4243–4247, 2022. doi: 10.1109/ICASSP43922.2022.9746778.
- [52] Yibo Yang, Shixiang Chen, Xiangtai Li, Liang Xie, Zhouchen Lin, and Dacheng Tao. Inducing neural collapse in imbalanced learning: Do we really need a learnable classifier at the end of deep neural network?, 2022. URL <https://arxiv.org/abs/2203.09081v3>.
- [53] Tom Tirer and Joan Bruna. Extended unconstrained features model for exploring deep neural collapse. In Kamalika Chaudhuri, Stefanie Jegelka, Le Song, Csaba Szepesvari, Gang Niu, and Sivan Sabato, editors, *Proceedings of the 39th International Conference on Machine Learning*, volume 162 of *Proceedings of Machine Learning Research*, pages 21478–21505. PMLR, 17–23 Jul 2022. URL <https://proceedings.mlr.press/v162/tirer22a.html>.
- [54] Peng Wang, Huikang Liu, Can Yaras, Laura Balzano, and Qing Qu. Linear convergence analysis of neural collapse with unconstrained features. In *OPT 2022: Optimization for Machine Learning (NeurIPS 2022 Workshop)*, 2022.
- [55] Jinxin Zhou, Chong You, Xiao Li, Kangning Liu, Sheng Liu, Qing Qu, and Zhihui Zhu. Are all losses created equal: A neural collapse perspective, 2022. URL <https://arxiv.org/abs/2210.02192v2>.
- [56] Akshay Rangamani, Marius Lindegaard, Tomer Galanti, and Tomaso A Poggio. Feature learning in deep classifiers through intermediate neural collapse. In Andreas Krause, Emma Brunskill, Kyunghyun Cho, Barbara Engelhardt, Sivan Sabato, and Jonathan Scarlett, editors, *Proceedings of the 40th International Conference on Machine Learning*, volume 202 of *Proceedings of Machine Learning Research*, pages 28729–28745. PMLR, 23–29 Jul 2023. URL <https://proceedings.mlr.press/v202/rangamani23a.html>.
- [57] Tom Tirer, Haoxiang Huang, and Jonathan Niles-Weed. Perturbation analysis of neural collapse. In *International Conference on Machine Learning*, pages 34301–34329. PMLR, 2023.
- [58] Hien Dang, Tho Tran, Stanley Osher, Hung Tran-The, Nhat Ho, and Tan Nguyen. Neural collapse in deep linear networks: From balanced to imbalanced data, 2023. URL <https://arxiv.org/abs/2301.00437v5>.
- [59] Peter Súkeník, Marco Mondelli, and Christoph H Lampert. Deep neural collapse is provably optimal for the deep unconstrained features model. *Advances in Neural Information Processing Systems*, 36, 2024.

- [60] Duc Anh Nguyen, Ron Levie, Julian Lienen, Eyke Hüllermeier, and Gitta Kutyniok. Memorization-dilation: Modeling neural collapse under noise. In *The Eleventh International Conference on Learning Representations*, 2023. URL <https://openreview.net/forum?id=cJWxqmmDL2b>.
- [61] Zhisheng Zhong, Jiequan Cui, Yibo Yang, Xiaoyang Wu, Xiaojuan Qi, Xiangyu Zhang, and Jiaya Jia. Understanding imbalanced semantic segmentation through neural collapse. In *Proceedings of the IEEE/CVF Conference on Computer Vision and Pattern Recognition*, pages 19550–19560, 2023.
- [62] Xuantong Liu, Jianfeng Zhang, Tianyang Hu, He Cao, Yuan Yao, and Lujia Pan. Inducing neural collapse in deep long-tailed learning. In *International Conference on Artificial Intelligence and Statistics*, pages 11534–11544. PMLR, 2023.
- [63] Peifeng Gao, Qianqian Xu, Peisong Wen, Huiyang Shao, Zhiyong Yang, and Qingming Huang. A study of neural collapse phenomenon: Grassmannian frame, symmetry and generalization, 2023. URL <https://arxiv.org/abs/2304.08914v2>.
- [64] Mufan Bill Li, Mihai Nica, and Daniel M. Roy. The neural covariance sde: Shaped infinite depth-and-width networks at initialization, 2023. URL <https://arxiv.org/abs/2206.02768v3>.
- [65] Zhanxuan Hu, Yichen Wang, Hailong Ning, Yonghang Tai, and Feiping Nie. Neural collapse inspired semi-supervised learning with fixed classifier. *Information Sciences*, 667:120469, 2024.
- [66] Gao Peifeng, Qianqian Xu, Yibo Yang, Peisong Wen, Huiyang Shao, Zhiyong Yang, Bernard Ghanem, and Qingming Huang. Towards demystifying the generalization behaviors when neural collapse emerges, 2024. URL <https://openreview.net/forum?id=XVv4S6LnMk>.
- [67] Nelson Elhage, Tristan Hume, Catherine Olsson, Nicholas Schiefer, Tom Henighan, Shauna Kravec, Zac Hatfield-Dodds, Robert Lasenby, Dawn Drain, Carol Chen, Roger Grosse, Sam McCandlish, Jared Kaplan, Dario Amodei, Martin Wattenberg, and Christopher Olah. Toy models of superposition. *Transformer Circuits Thread*, 2022. URL https://transformer-circuits.pub/2022/toy_model/index.html.
- [68] Alec Radford, Jeff Wu, Rewon Child, David Luan, Dario Amodei, and Ilya Sutskever. Language models are unsupervised multitask learners. 2019.
- [69] A. Dubey et al. (101 additional authors). The llama 3 herd of models. 2024. URL <https://arxiv.org/abs/2407.21783>. All authors were affiliated with Meta.
- [70] Christos Thrampoulidis, Ganesh Ramachandra Kini, Vala Vakilian, and Tina Behnia. Imbalance trouble: Revisiting neural-collapse geometry. *Advances in Neural Information Processing Systems*, 35:27225–27238, 2022.
- [71] Nagarajan Natarajan, Inderjit S Dhillon, Pradeep K Ravikumar, and Ambuj Tewari. Learning with noisy labels. *Advances in neural information processing systems*, 26, 2013.
- [72] Quinn Fisher, Haoming Meng, and Vardan Papyan. Pushing boundaries: Mixup’s influence on neural collapse, 2024. URL <https://arxiv.org/abs/2402.06171v1>.
- [73] Pengyu Li, Xiao Li, Yutong Wang, and Qing Qu. Neural collapse in multi-label learning with pick-all-label loss, 2024. URL <https://arxiv.org/abs/2310.15903v4>.
- [74] Kaiming He, Xiangyu Zhang, Shaoqing Ren, and Jian Sun. Deep residual learning for image recognition. In *Proceedings of the IEEE conference on computer vision and pattern recognition*, pages 770–778, 2016.
- [75] David Mimno and Laure Thompson. The strange geometry of skip-gram with negative sampling. In Martha Palmer, Rebecca Hwa, and Sebastian Riedel, editors, *Proceedings of the 2017 Conference on Empirical Methods in Natural Language Processing*, pages 2873–2878, Copenhagen, Denmark, September 2017. Association for Computational Linguistics. doi: 10.18653/v1/D17-1308. URL <https://aclanthology.org/D17-1308>.

- [76] Kawin Ethayarajh. How contextual are contextualized word representations? comparing the geometry of bert, elmo, and gpt-2 embeddings, 2019. URL <https://arxiv.org/abs/1909.00512>.
- [77] Alex Wang, Amanpreet Singh, Julian Michael, Felix Hill, Omer Levy, and Samuel R. Bowman. Glue: A multi-task benchmark and analysis platform for natural language understanding, 2019. URL <https://arxiv.org/abs/1804.07461v3>.
- [78] Jia Hui Feng, Edmund M-K Lai, and Weihua Li. A study of neural collapse for text classification. In *International Conference on Deep Learning Theory and Applications*, pages 126–142. Springer, 2023.
- [79] Thomas Laurent, James H. von Brecht, and Xavier Bresson. Feature collapse, 2023. URL <https://arxiv.org/abs/2305.16162v1>.
- [80] Sid Black, Leo Gao, Phil Wang, Connor Leahy, and Stella Biderman. GPT-Neo: Large Scale Autoregressive Language Modeling with Mesh-Tensorflow, March 2021. URL <https://doi.org/10.5281/zenodo.5297715>. If you use this software, please cite it using these metadata.
- [81] Tom Brown, Benjamin Mann, Nick Ryder, Melanie Subbiah, Jared D Kaplan, Prafulla Dhariwal, Arvind Neelakantan, Pranav Shyam, Girish Sastry, Amanda Askell, et al. Language models are few-shot learners. *Advances in neural information processing systems*, 33:1877–1901, 2020.
- [82] Susan Zhang, Stephen Roller, Naman Goyal, Mikel Artetxe, Moya Chen, Shuhui Chen, Christopher Dewan, Mona Diab, Xian Li, Xi Victoria Lin, Todor Mihaylov, Myle Ott, Sam Shleifer, Kurt Shuster, Daniel Simig, Punit Singh Koura, Anjali Sridhar, Tianlu Wang, and Luke Zettlemoyer. Opt: Open pre-trained transformer language models, 2022. URL <https://arxiv.org/abs/2205.01068v4>.
- [83] Hugo Touvron, Thibaut Lavril, Gautier Izacard, Xavier Martinet, Marie-Anne Lachaux, Timothée Lacroix, Baptiste Rozière, Naman Goyal, Eric Hambro, Faisal Azhar, Aurelien Rodriguez, Armand Joulin, Edouard Grave, and Guillaume Lample. Llama: Open and efficient foundation language models, 2023. URL <https://arxiv.org/abs/2302.13971v1>.
- [84] Albert Q. Jiang, Alexandre Sablayrolles, Arthur Mensch, Chris Bamford, Devendra Singh Chaplot, Diego de las Casas, Florian Bressand, Gianna Lengyel, Guillaume Lample, Lucile Saulnier, Lélio Renard Lavaud, Marie-Anne Lachaux, Pierre Stock, Teven Le Scao, Thibaut Lavril, Thomas Wang, Timothée Lacroix, and William El Sayed. Mistral 7b, 2023. URL <https://arxiv.org/abs/2310.06825v1>.
- [85] Ronald A Fisher. The use of multiple measurements in taxonomic problems. *Annals of eugenics*, 7(2):179–188, 1936.
- [86] C Radhakrishna Rao. The utilization of multiple measurements in problems of biological classification. *Journal of the Royal Statistical Society. Series B (Methodological)*, 10(2):159–203, 1948.
- [87] Thomas Strohmer and Robert W Heath Jr. Grassmannian frames with applications to coding and communication. *Applied and computational harmonic analysis*, 14(3):257–275, 2003.
- [88] Shayne FD Waldron. *An introduction to finite tight frames*. Springer, 2018.
- [89] David L Donoho, Michael Elad, and Vladimir N Temlyakov. Stable recovery of sparse overcomplete representations in the presence of noise. *IEEE Transactions on information theory*, 52(1):6–18, 2005.
- [90] Joel A Tropp. Just relax: Convex programming methods for identifying sparse signals in noise. *IEEE transactions on information theory*, 52(3):1030–1051, 2006.
- [91] Daniel M. Ziegler, Nisan Stiennon, Jeffrey Wu, Tom B. Brown, Alec Radford, Dario Amodei, Paul Christiano, and Geoffrey Irving. Fine-tuning language models from human preferences, 2020. URL <https://arxiv.org/abs/1909.08593>.

- [92] Rafael Rafailov, Archit Sharma, Eric Mitchell, Christopher D Manning, Stefano Ermon, and Chelsea Finn. Direct preference optimization: Your language model is secretly a reward model. In A. Oh, T. Naumann, A. Globerson, K. Saenko, M. Hardt, and S. Levine, editors, *Advances in Neural Information Processing Systems*, volume 36, pages 53728–53741. Curran Associates, Inc., 2023. URL https://proceedings.neurips.cc/paper_files/paper/2023/file/a85b405ed65c6477a4fe8302b5e06ce7-Paper-Conference.pdf.
- [93] Vardan Papyan. Traces of class/cross-class structure pervade deep learning spectra, 2020. URL <https://arxiv.org/abs/2008.11865v1>.
- [94] Christopher R. Hoyt and Art B. Owen. Probing neural networks with t-sne, class-specific projections and a guided tour, 2021. URL <https://arxiv.org/abs/2107.12547v1>.
- [95] John Zarka, Florentin Guth, and Stéphane Mallat. Separation and concentration in deep networks, 2021. URL <https://arxiv.org/abs/2012.10424v2>.
- [96] Ido Ben-Shaul and Shai Dekel. Nearest class-center simplification through intermediate layers. In Alexander Cloninger, Timothy Doster, Tegan Emerson, Manohar Kaul, Ira Ktena, Henry Kvinge, Nina Miolane, Bastian Rieck, Sarah Tymochko, and Guy Wolf, editors, *Proceedings of Topological, Algebraic, and Geometric Learning Workshops 2022*, volume 196 of *Proceedings of Machine Learning Research*, pages 37–47. PMLR, 25 Feb–22 Jul 2022. URL <https://proceedings.mlr.press/v196/ben-shaul22a.html>.
- [97] Hangfeng He and Weijie J. Su. A law of data separation in deep learning, 2022. URL <https://arxiv.org/abs/2210.17020v2>.
- [98] Liam Parker, Emre Onal, Anton Stengel, and Jake Intrater. Neural collapse in the intermediate hidden layers of classification neural networks, 2023. URL <https://arxiv.org/abs/2308.02760v1>.
- [99] Wojciech Masarczyk, Mateusz Ostaszewski, Ehsan Imani, Razvan Pascanu, Piotr Mił oś, and Tomasz Trzcinski. The tunnel effect: Building data representations in deep neural networks. In A. Oh, T. Naumann, A. Globerson, K. Saenko, M. Hardt, and S. Levine, editors, *Advances in Neural Information Processing Systems*, volume 36, pages 76772–76805. Curran Associates, Inc., 2023. URL https://proceedings.neurips.cc/paper_files/paper/2023/file/f249db9ab5975586f36df46f8958c008-Paper-Conference.pdf.
- [100] Daniel Beaglehole, Peter Súkeník, Marco Mondelli, and Mikhail Belkin. Average gradient outer product as a mechanism for deep neural collapse, 2024. URL <https://arxiv.org/abs/2402.13728v2>.
- [101] Peng Wang, Xiao Li, Can Yaras, Zhihui Zhu, Laura Balzano, Wei Hu, and Qing Qu. Understanding deep representation learning via layerwise feature compression and discrimination, 2024. URL <https://arxiv.org/abs/2311.02960v2>.
- [102] Sicong Wang, Kuo Gai, and Shihua Zhang. Progressive feedforward collapse of resnet training, 2024. URL <https://arxiv.org/abs/2405.00985v1>.
- [103] Connall Garrod and Jonathan P. Keating. Unifying low dimensional observations in deep learning through the deep linear unconstrained feature model, 2024. URL <https://arxiv.org/abs/2404.06106v1>.
- [104] Emanuele Zangrandi, Piero Deidda, Simone Brugiapaglia, Nicola Guglielmi, and Francesco Tudisco. Neural rank collapse: Weight decay and small within-class variability yield low-rank bias, 2024. URL <https://arxiv.org/abs/2402.03991v1>.
- [105] Jiachen Jiang, Jinxin Zhou, and Zhihui Zhu. On layer-wise representation similarity: Application for multi-exit models with a single classifier, 2024. URL <https://arxiv.org/abs/2406.14479>.
- [106] Mengjia Xu, Akshay Rangamani, Qianli Liao, Tomer Galanti, and Tomaso Poggio. Dynamics in deep classifiers trained with the square loss: Normalization, low rank, neural collapse, and generalization bounds. *Research*, 6:0024, 2023.

- [107] Tong Liang and Jim Davis. Inducing neural collapse to a fixed hierarchy-aware frame for reducing mistake severity. In *Proceedings of the IEEE/CVF International Conference on Computer Vision*, pages 1443–1452, 2023.
- [108] Guglielmo Bonifazi, Iason Chalas, Gian Hess, and Jakub Łucki. Can we understand plasticity through neural collapse?, 2024. URL <https://arxiv.org/abs/2404.02719v1>.
- [109] Dan Hendrycks, Collin Burns, Steven Basart, Andy Zou, Mantas Mazeika, Dawn Song, and Jacob Steinhardt. Measuring massive multitask language understanding. *Proceedings of the International Conference on Learning Representations (ICLR)*, 2021.
- [110] BIG bench authors. Beyond the imitation game: Quantifying and extrapolating the capabilities of language models. *Transactions on Machine Learning Research*, 2023. ISSN 2835-8856. URL <https://openreview.net/forum?id=uyTL5Bvosj>.
- [111] Zhengxiao Du, Aohan Zeng, Yuxiao Dong, and Jie Tang. Understanding emergent abilities of language models from the loss perspective, 2024. URL <https://arxiv.org/abs/2403.15796>.
- [112] Yuzhen Huang, Jinghan Zhang, Zifei Shan, and Junxian He. Compression represents intelligence linearly. In *First Conference on Language Modeling*, 2024. URL <https://openreview.net/forum?id=SHMj84U5SH>.
- [113] Mingjia Yin, Chuhan Wu, Yufei Wang, Hao Wang, Wei Guo, Yasheng Wang, Yong Liu, Ruiming Tang, Defu Lian, and Enhong Chen. Entropy law: The story behind data compression and llm performance, 2024.
- [114] Li Guo, Keith Ross, Zifan Zhao, George Andriopoulos, Shuyang Ling, Yufeng Xu, and Zixuan Dong. Cross entropy versus label smoothing: A neural collapse perspective, 2024. URL <https://arxiv.org/abs/2402.03979v2>.
- [115] Jingxuan Xu, Wuyang Chen, Linyi Li, Yao Zhao, and Yunchao Wei. Collapsed language models promote fairness, 2024. URL <https://arxiv.org/abs/2410.04472>.
- [116] Stephen Merity, Ilya Sutskever, Simon Kornblith, and Nikhil Goyal. Pointer sentinel mixture models. *arXiv preprint arXiv:1609.07843*, 2016.
- [117] Yao Zhu, Zhen Yu, Chao Zhang, Yijia Wu, et al. Aligning books and movies: Towards story-like visual explanations by watching movies and reading books. *arXiv preprint arXiv:1506.05829*, 2015.
- [118] Common Crawl. Common crawl, 2023. URL <https://commoncrawl.org>. Accessed: 2023-10-30.
- [119] Leo Gao, Stella Biderman, Sid Black, Laurence Golding, Travis Hoppe, Charles Foster, Jason Phang, Horace He, Anish Thite, Noa Nabeshima, Shawn Presser, and Connor Leahy. The pile: An 800gb dataset of diverse text for language modeling, 2020. URL <https://arxiv.org/abs/2101.00027>.
- [120] Ilia Shumailov, Zakhar Shumaylov, Yiren Zhao, Yarin Gal, Nicolas Papernot, and Ross Anderson. The curse of recursion: Training on generated data makes models forget, 2024. URL <https://arxiv.org/abs/2305.17493>.
- [121] Matthias Gerstgrasser, Rylan Schaeffer, Apratim Dey, Rafael Rafailov, Henry Sleight, John Hughes, Tomasz Korbak, Rajashree Agrawal, Dhruv Pai, Andrey Gromov, Daniel A. Roberts, Diyi Yang, David L. Donoho, and Sanmi Koyejo. Is model collapse inevitable? breaking the curse of recursion by accumulating real and synthetic data, 2024. URL <https://arxiv.org/abs/2404.01413>.
- [122] Neil Burgess, Jelena Milanovic, Nigel Stephens, Konstantinos Monachopoulos, and David Mansell. Bfloat16 processing for neural networks. In *2019 IEEE 26th Symposium on Computer Arithmetic (ARITH)*, pages 88–91, 2019. doi: 10.1109/ARITH.2019.00022.

A Dataset

TinyStories is a dataset of short children’s stories generated by GPT-3.5 and GPT-4 [2], released with the CDLA-Sharing-1.0 licence. We trained and evaluated models on their first version, as described:

- The 2,141,709 stories are split into 2,119,719 train and 21,990 validation stories.
- Their experimental setup [2] called for the GPT-2 [68] tokenizer, of which only a subset vocabulary $\mathbb{V} = \llbracket 1, 29233 \rrbracket$ appears in TinyStories.
- Following the GPT-style teacher-forcing regime for training/evaluation [8], raw sequences (stories) from the train set are packed (by two preprocessing workers) into 229,367 (S) chunks of 2048 (T) tokens each. This setup provides 469,514,249 (N) ground-truth¹⁸ token samples for training.

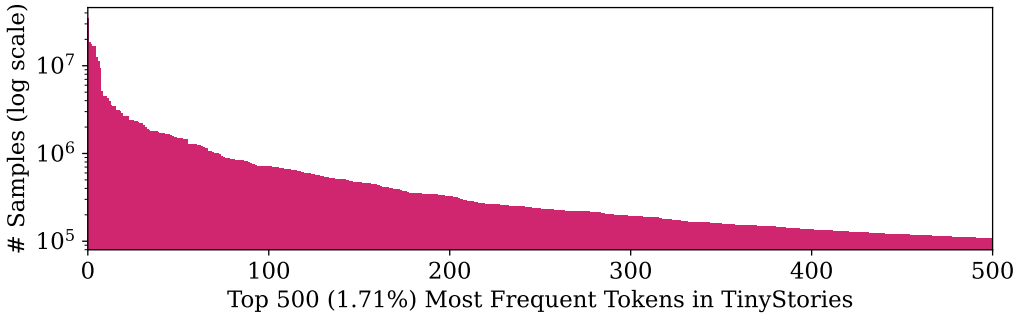


Figure 4: The 500 most frequent classes from TinyStories [2] exhibit significant sample imbalance. Despite the synthetic nature of TinyStories, such a distribution is typical of natural language [11, 12].

A.1 Alternative (Real) Datasets

The study of \mathcal{NC} in causal language modelling at the token level would be unreasonably expensive, so the motivation to use a small dataset is clear. However, most commonly used text datasets such as WikiText [116], BookCorpus [117], CommonCrawl [118], or most subsets from the Pile [119] are much too complex and broad to be effectively compressed by CLMs of the scale that we work with.

WikiText-2 and WikiText-103 present significant drawbacks for our experiments. Both datasets contain a considerable amount of low-quality data that does not concentrate on essential linguistic structures such as grammar, vocabulary, facts, and reasoning. WikiText-2 has a similar empirical vocabulary to TinyStories under the GPT-Neo [80] tokenizer (27K vs. 29K) but only has around 34K rows of training data compared to 2.1M in TinyStories. Our small-scale NC experiment on WikiText-2 revealed that the models were very brittle and prone to overfitting. On the other hand, WikiText-103 is comparably sized to TinyStories but utilizes around 44K unique tokens. Our CLMs trained on WikiText-103 struggled to produce coherent sentences, likely due to the excessive breadth and information, as noted by the authors of TinyStories. Beyond these two, we were unable to find any real datasets that both followed established scaling laws [14, 15] for CLMs at our scale and are simple enough to suit the analysis of \mathcal{NC} .

A.2 On the Use of TinyStories

According to its authors, TinyStories [2] is explicitly designed to preserve the essential elements of natural language, such as grammar, vocabulary, facts, and reasoning, while being smaller and more refined in terms of its breadth and diversity. Unlike large corpora that can overwhelm small language models (SLMs) due to their excessive breadth and diversity, TinyStories offers a concentrated dataset that hones in on core linguistic structures and reasoning capabilities. This is evident in its small vocabulary, consisting of approximately 1500 words that a child would use, and in its 29K empirical vocabulary under the GPT-Neo tokenizer.

¹⁸ $N = S(T - 1)$ as we cannot use the first ground-truth nor the last predicted token in any chunk.

Despite its concentrated nature, TinyStories enables models trained on it to produce grammatically correct, factual, and reasonable stories. Additionally, these models can be finetuned on specific instructions found in the TinyStories-Instruct dataset. The authors of TinyStories also demonstrate that their models can creatively produce stories dissimilar enough to their training data, indicating a balanced capability for generalization and creativity.

One particular advantage of TinyStories is the small vocabulary relative to total training tokens, rendering a reasonable number of classes with higher average token counts. This is relevant because the possibility of \mathcal{NC} and a CLM’s ability to compress language data into distinct geometries depend partially on the ratios between embedding dimension, vocabulary size, and average token frequency. Conveniently, frequency analysis of the overall dataset produced a distribution (Figure 4) similar to real human language, so TinyStories should provide a good balance for an initial study of this \mathcal{NC} .

Additionally, TinyStories has a more regular structure as GPT-3.5/4 was instructed to produce children’s stories with certain themes and forms with a conservative vocabulary. We believe this would reduce the amount of clustering noise from the breadth of information and structures in real general data, and allow our smaller CLMs to exhibit some clear trends toward \mathcal{NC} .

Furthermore, TinyStories was created using GPT 3.5/4, advanced language models with significantly larger architectures trained on orders of magnitude more tokens; this should help minimize the effect of the synthetic nature of the generated dataset. We also considered a possible effect of model collapse as a result of training on synthetic data [120] and follow-up work [121] suggest that a single iteration of data generation (as generated TinyStories) has a very negligible model collapse.

B Model Architectural Details

Table 2: Sample architectural configuration for a 12-layer 1024-dimensional causal language model (CLM) based on [2] and GPT-Neo [80]. Shallower models have configurations with `attention_layers` and `attention_types` truncated. Narrower models adjust `hidden_size` to their width (d). All other configuration values are the same across models.

SETTING	VALUE
<code>activation_function</code>	<code>gelu_new</code>
<code>architectures</code>	<code>GPTNeoForCausalLM</code>
<code>attention_dropout</code>	0
<code>attention_layers</code>	<code>global, local, global, local, ...</code>
<code>attention_types</code>	<code>[[global, local], 6]</code>
<code>bos_token_id</code>	50256
<code>embed_dropout</code>	0
<code>eos_token_id</code>	50256
<code>gradient_checkpointing</code>	<code>false</code>
<code>hidden_size</code>	1024
<code>initializer_range</code>	0.02
<code>intermediate_size</code>	<code>null</code>
<code>layer_norm_epsilon</code>	<code>1e-05</code>
<code>max_position_embeddings</code>	2048
<code>model_type</code>	<code>gpt_neo</code>
<code>num_heads</code>	16
<code>num_layers</code>	12
<code>resid_dropout</code>	0
<code>summary_activation</code>	<code>null</code>
<code>summary_first_dropout</code>	0.1
<code>summary_proj_to_labels</code>	<code>true</code>
<code>summary_type</code>	<code>cls_index</code>
<code>summary_use_proj</code>	<code>true</code>
<code>torch_dtype</code>	<code>float32</code>
<code>transformers_version</code>	4.28.1
<code>use_cache</code>	<code>true</code>
<code>vocab_size</code>	50257
<code>window_size</code>	256

C Optimization

The training was performed using an adaptation of an open-source causal language modelling script from Huggingface: https://github.com/huggingface/transformers/blob/main/examples/pytorch/language-modeling/run_clm.py

- Each model was trained on a single NVIDIA A100 (40GB) GPU for up to 8 hours per epoch.
- Learning rates were set by a linear schedule based on the number of steps with no warm-up.
- Training was performed in `bfloat16` [122] mixed precision.
- The results presented in this work are from two sets of models trained with weight decay $\beta = 0.0005$ [51] and $\beta = 0.1$ [81]. A previous set of models was trained without weight decay and the results are very similar to $\beta = 0.0005$.

Table 3: Batch sizes used to train models on a single NVIDIA A100 (40GB) GPU. Width (d) and depth (L) correspond to `hidden_size` and length of `attention_layers`, respectively, in Table 2.

DEPTH (L) ↓	WIDTH (d) →	64	128	256	512	768	1024
1-layer		16	16	16	16	16	16
2-layer		16	16	16	16	16	8
4-layer		8	8	8	8	8	8
8-layer		8	8	8	4	4	4
12-layer		4	4	4	4	4	4

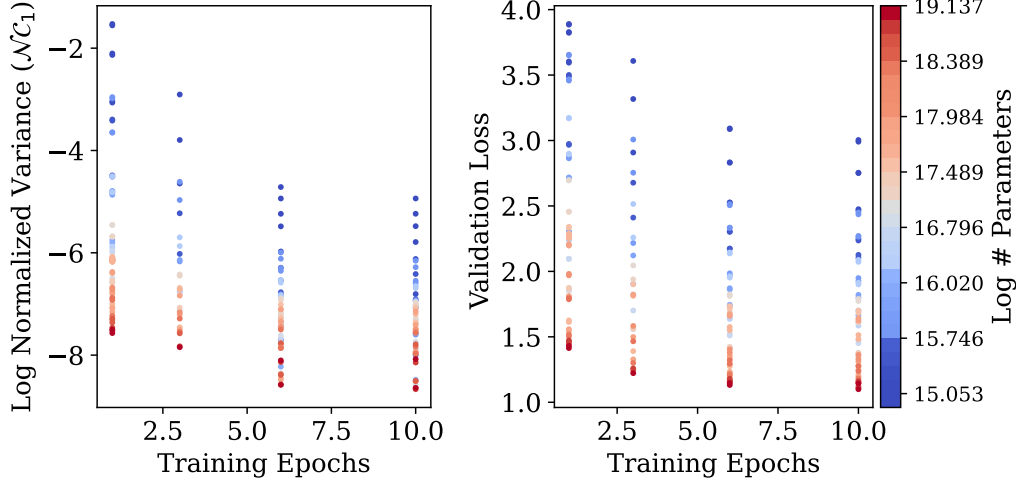


Figure 5: Average (logarithmic) class-distance normalized variance (CDNV, $\mathcal{N}\mathcal{C}_1$) (left) and validation (cross-entropy) loss (right) with respect to training epochs.

D Embeddings Collection & \mathcal{NC} Analysis

Codes for (post-)training analysis are hosted on GitHub:

- Main code <https://github.com/rhubarbwu/linguistic-collapse>
- Auxillary package: <https://github.com/rhubarbwu/neural-collapse>

One pass over the train set for embeddings collection can take up to 6 hours on a single NVIDIA A100 (40GB) GPU. Analysis of a single metric for a given model takes less than 5 minutes.

E Within-Class Variability Collapse with Scale — \mathcal{NC}_1

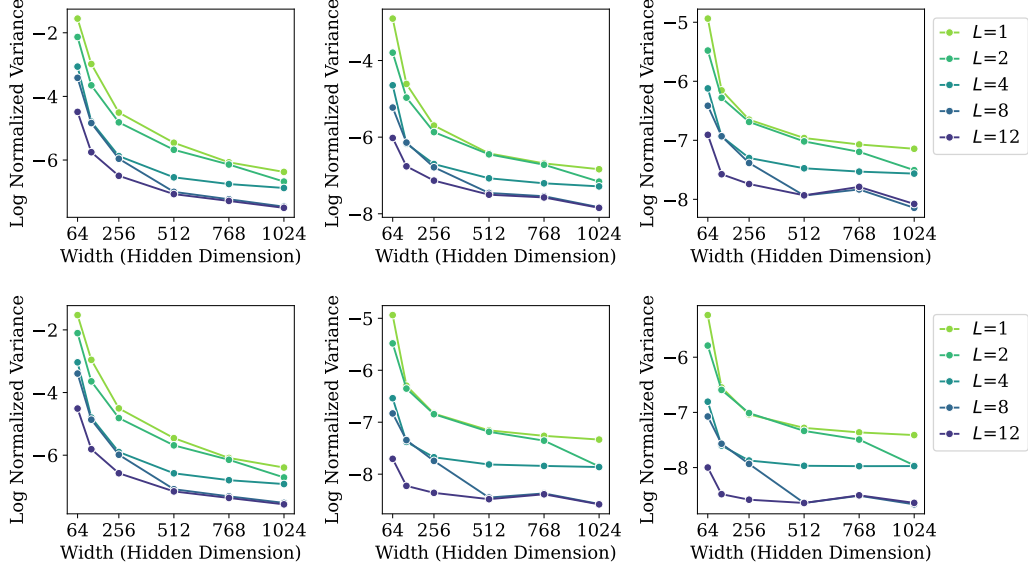


Figure 6: Average (logarithmic) class-distance normalized variance (CDNV) is reduced (\mathcal{NC}_1) when scaling width (d) and across training for 1 (left) through 10 (right) epochs with weight decays $\beta = 0.0005$ (top) and $\beta = 0.1$ (bottom).

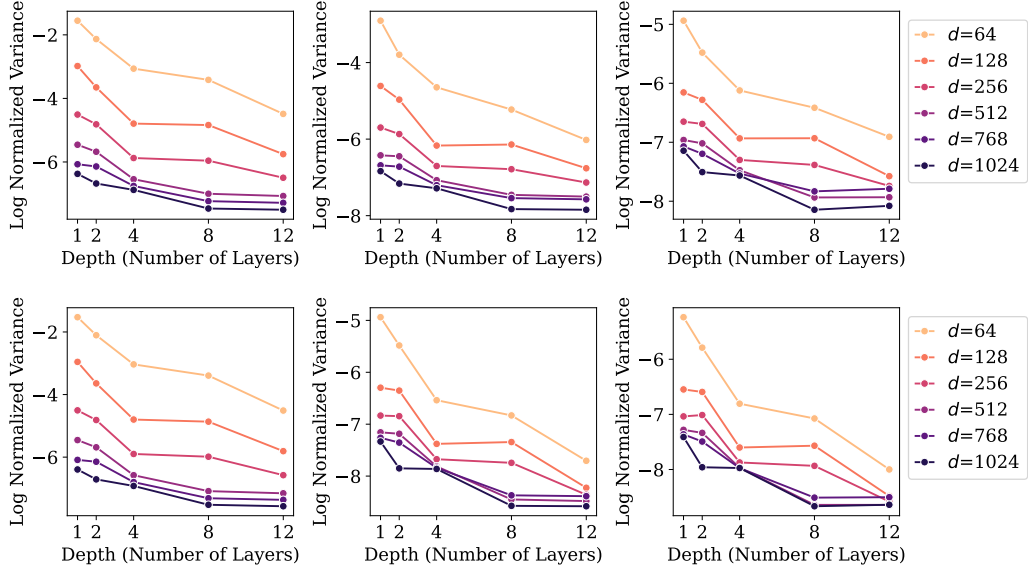


Figure 7: Average (logarithmic) class-distance normalized variance (CDNV) is reduced (\mathcal{NC}_1) when scaling depth (L) and across training for 1 (left) through 10 (right) epochs with weight decays $\beta = 0.0005$ (top) and $\beta = 0.1$ (bottom).

F Mean Norms Growth with Scale — (Related to \mathcal{NC}_2)

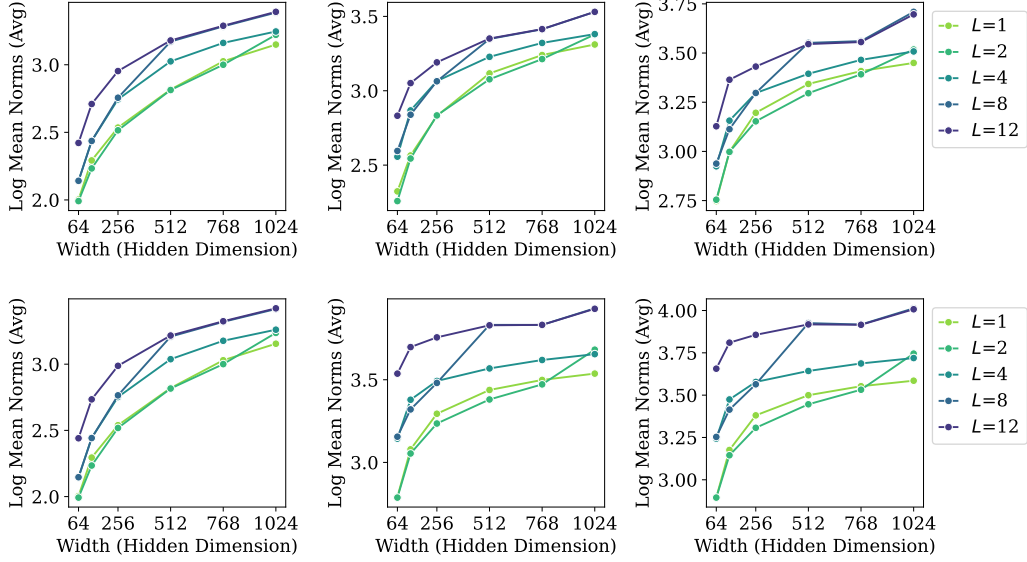


Figure 8: Logarithmic class mean norms grow when scaling width (d) and across training for 1 (left) through 10 (right) epochs with weight decays $\beta = 0.0005$ (top) and $\beta = 0.1$ (bottom).

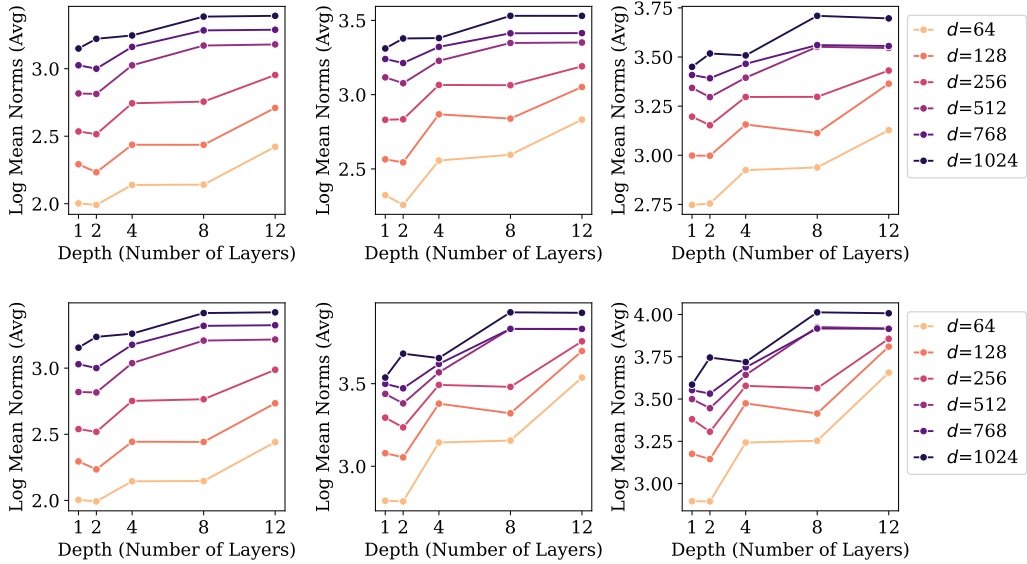


Figure 9: Logarithmic class mean norms grow when scaling depth (L) and across training for 1 (left) through 10 (right) epochs with weight decays $\beta = 0.0005$ (top) and $\beta = 0.1$ (bottom).

G Equinormness with Scale — $(\mathcal{G})\mathcal{NC}_2$

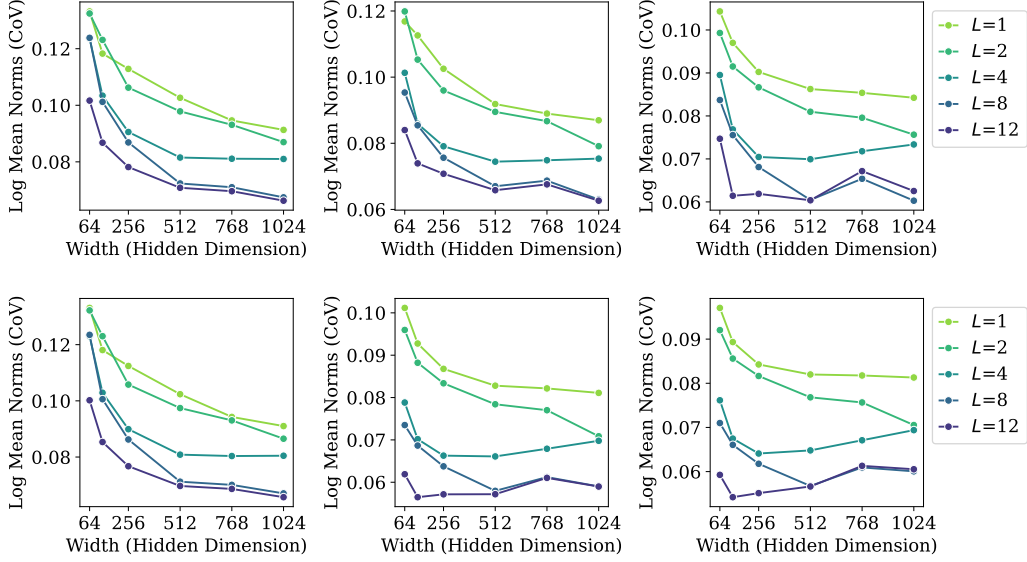


Figure 10: Variation in (logarithmic) norms decreases (\mathcal{NC}_2) when scaling width (d) in models trained for 1 (left) through 10 (right) with weight decays $\beta = 0.0005$ (top) and $\beta = 0.1$ (bottom). Note that the degree of equinormness eventually plateaus for sufficiently deep and trained models.

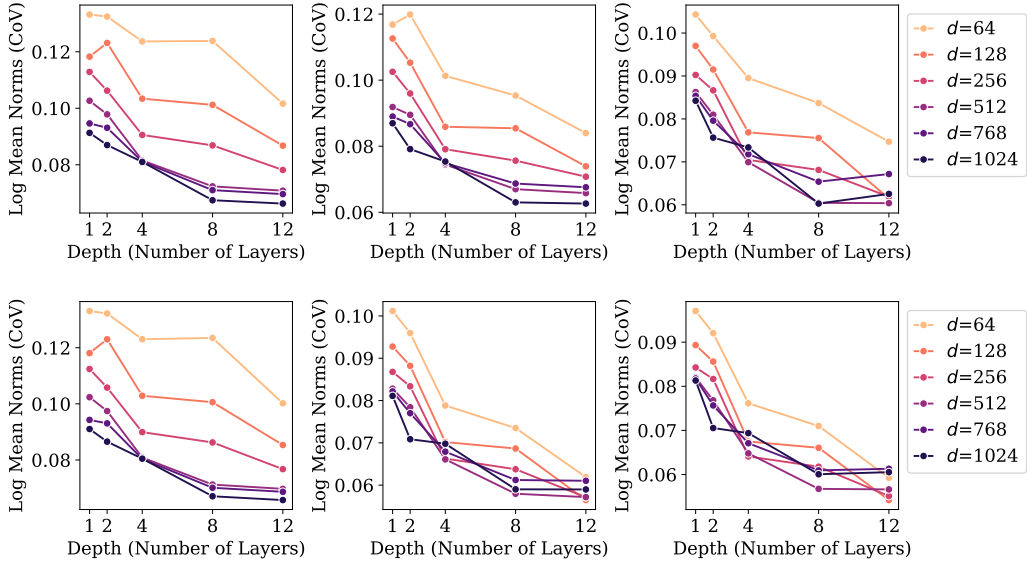


Figure 11: Variation in (logarithmic) norms decreases (\mathcal{NC}_2) when scaling depth (L) in models trained for 1 (left) through 10 (right) with weight decays $\beta = 0.0005$ (top) and $\beta = 0.1$ (bottom).

H Interference with Scale — (Related to \mathcal{NC}_2)

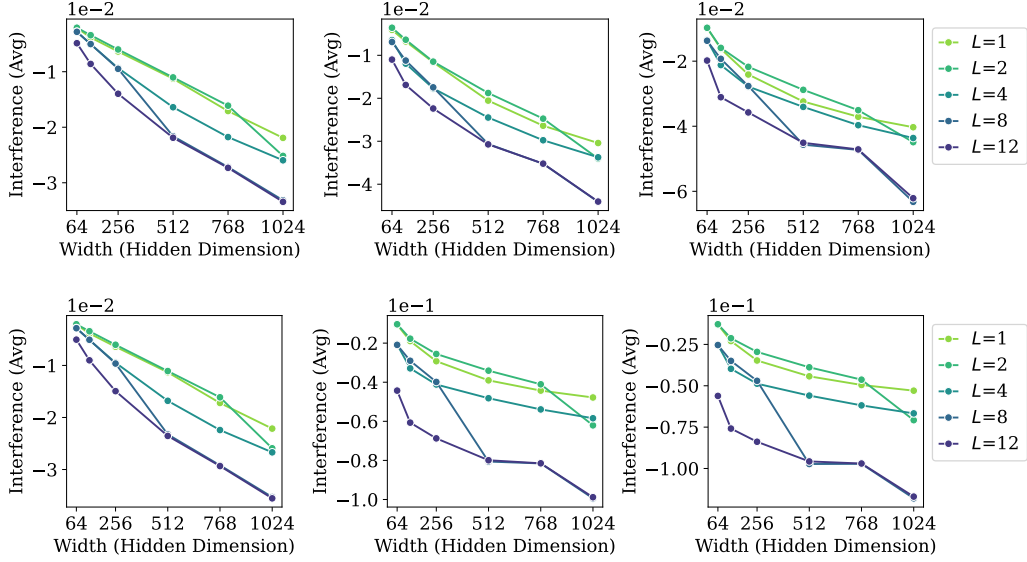


Figure 12: Average interference decreases (to some extent) when scaling width (d) in models trained for 1 (left) through 10 (right) with weight decays $\beta = 0.0005$ (top) and $\beta = 0.1$ (bottom).

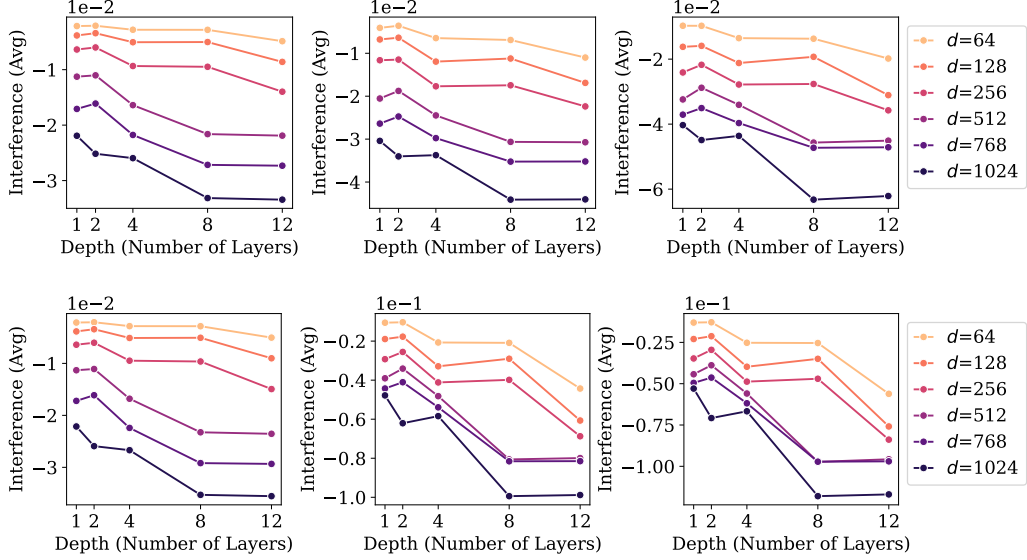


Figure 13: Average interference decreases (to some extent) when scaling depth (L) in models trained for 1 (left) through 10 (right) with weight decays $\beta = 0.0005$ (top) and $\beta = 0.1$ (bottom).

I Equiangularity with Scale — (Against \mathcal{NC}_2)

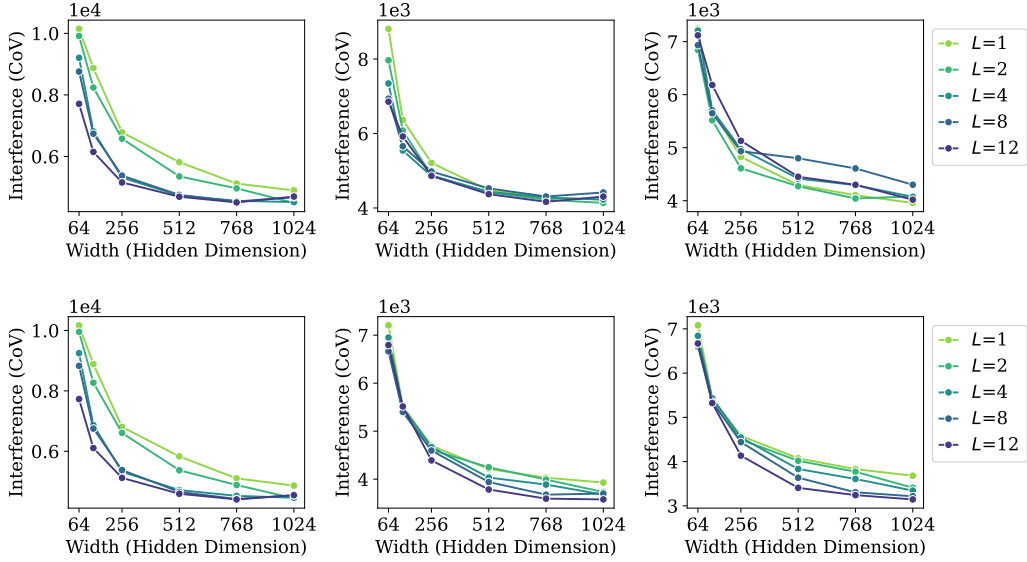


Figure 14: Variation in interference roughly increases when scaling width (d) in models trained for 1 (left) through 10 (right) with weight decays $\beta = 0.0005$ (top) and $\beta = 0.1$ (bottom). Note this trend is against equiangularity, affirming the traditional \mathcal{NC}_2 to be less useful than \mathcal{GNC}_2 [19].

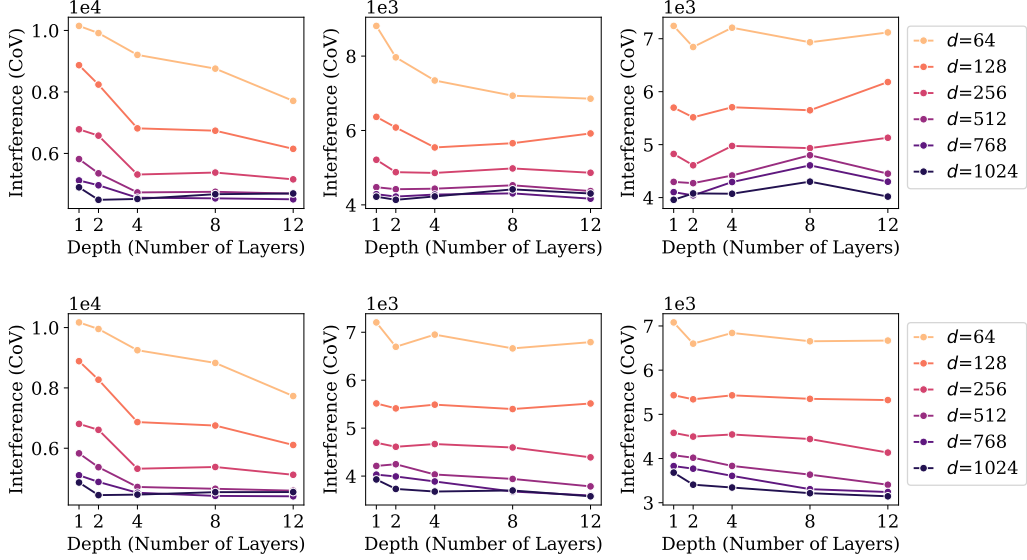


Figure 15: Variation in interference increases when scaling depth (L) in models trained for 1 (left) through 10 (right) with weight decays $\beta = 0.0005$ (top) and $\beta = 0.1$ (bottom). Note this trend is against equiangularity, affirming the traditional \mathcal{NC}_2 to be less useful than \mathcal{GNC}_2 [19].

J Logarithmic Distances with Scale — (Related to \mathcal{GNC}_2)

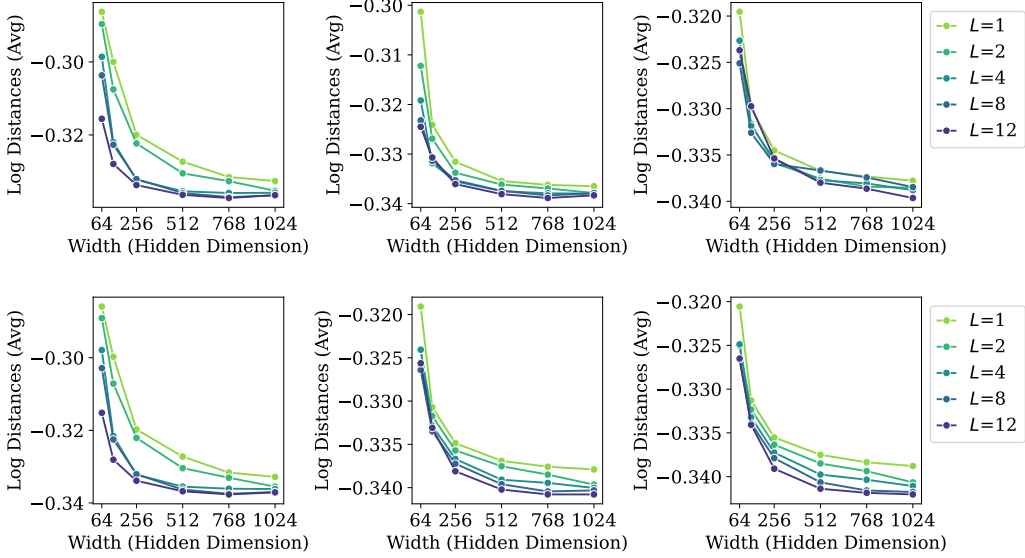


Figure 16: Average logarithmic distance decreases when scaling width (d) in models trained for 1 (left) through 10 (right) with weight decays $\beta = 0.0005$ (top) and $\beta = 0.1$ (bottom).

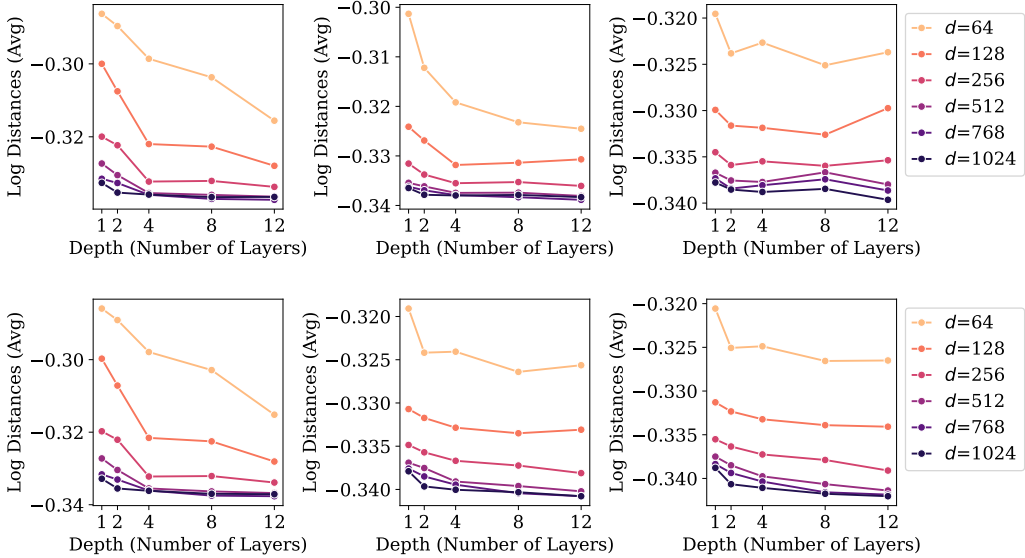


Figure 17: Average logarithmic distance decreases when scaling depth (L) in models trained for 1 (left) through 10 (right) with weight decays $\beta = 0.0005$ (top) and $\beta = 0.1$ (bottom).

K Hyperspherical Uniformity with Scale — \mathcal{GNC}_2

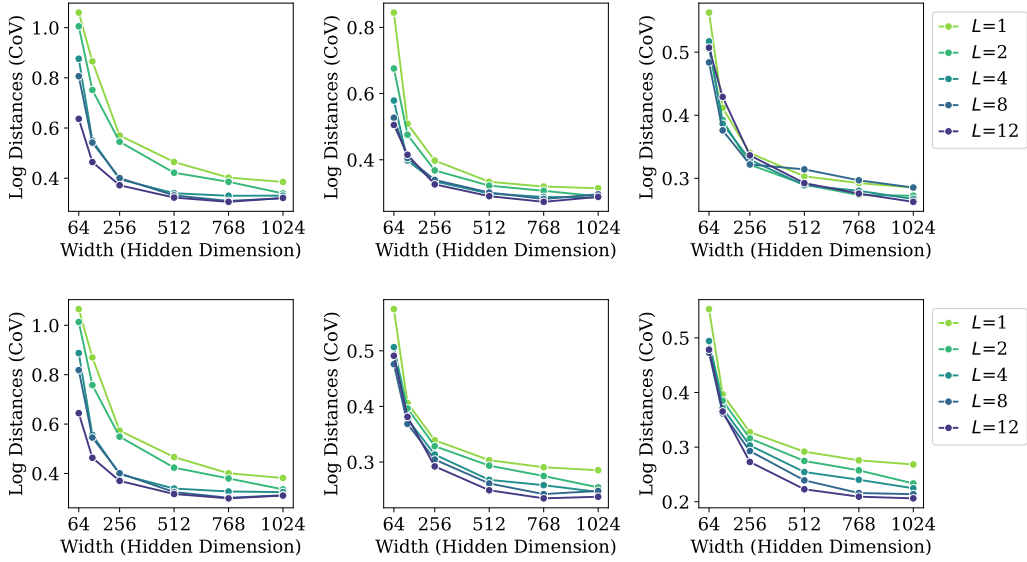


Figure 18: Variation in logarithmic distances decreases when scaling width (d) in models trained for 1 (left) through 10 (right) with weight decays $\beta = 0.0005$ (top) and $\beta = 0.1$ (bottom). This consistent trend towards hyperspherical uniformity affirms that \mathcal{GNC}_2 [19] is more useful than \mathcal{NC}_2 .

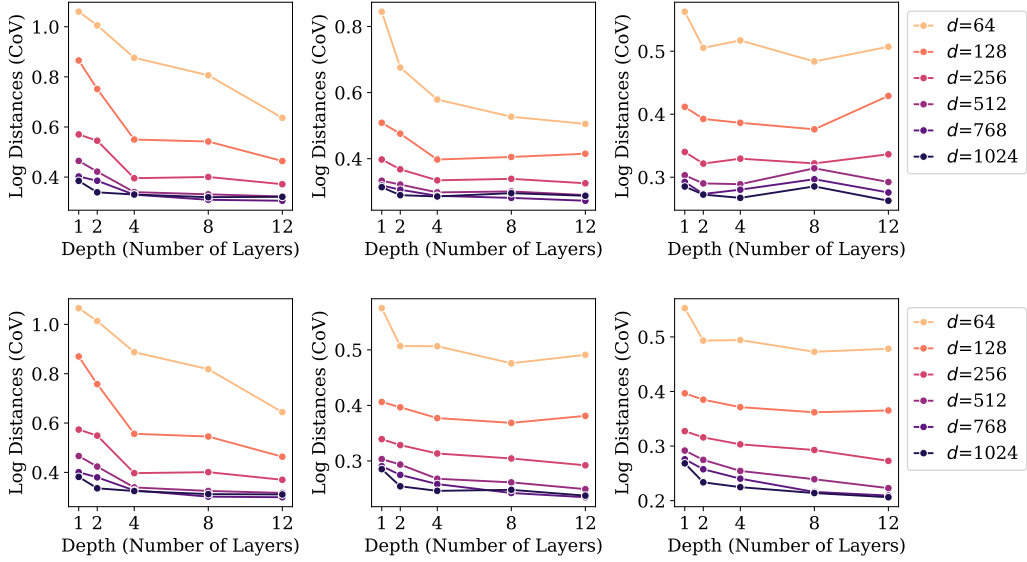


Figure 19: Variation in logarithmic distances decreases when scaling depth (L) in models trained for 1 (left) through 10 (right) with weight decays $\beta = 0.0005$ (top) and $\beta = 0.1$ (bottom). This consistent trend towards hyperspherical uniformity affirms that \mathcal{GNC}_2 [19] is more useful than \mathcal{NC}_2 .

L Correlations of $(\mathcal{G})\mathcal{NC}_2$ with Generalization Performance

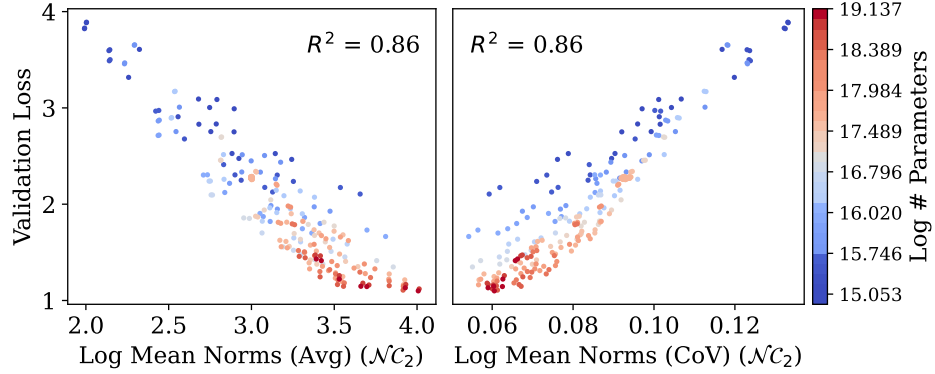


Figure 20: Generalization (validation loss) shows some correlation with logarithmic mean norms in both their average (left) and variations (i.e. equinormness, \mathcal{NC}_2) (right).

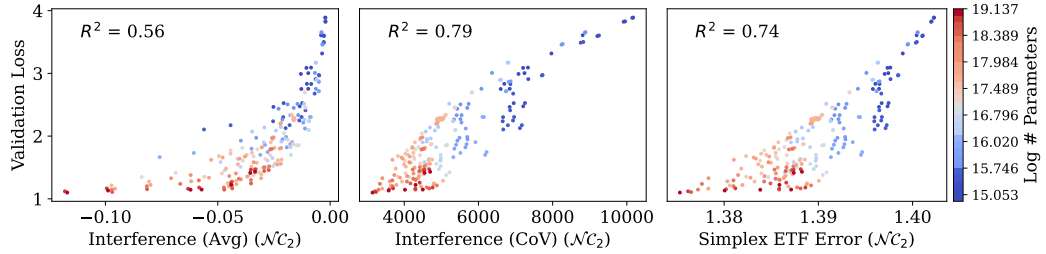


Figure 21: Generalization (validation loss) correlated with average interference (left) and its variation (i.e. equiangularity, \mathcal{NC}_2) (centre). We also computed the empirical measure from [5] (right).

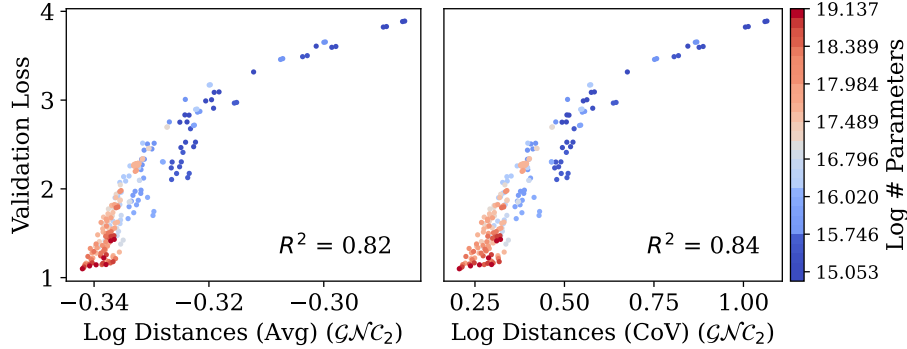


Figure 22: Validation loss shows some correlation with average (logarithmic) kernel distances and with their variation (i.e. hyperspherical uniformity, $G\mathcal{NC}_2$) (right).

M Self-Duality with Scale — (Against \mathcal{NC}_3)

Self-duality (\mathcal{NC}_3) was originally the convergence of classifiers to means up to rescaling [1]:

$$\left\| \frac{\mathbf{w}_c}{\|\mathbf{w}_c\|_2} - \frac{\boldsymbol{\mu}_c - \bar{\boldsymbol{\mu}}}{\|\boldsymbol{\mu}_c - \bar{\boldsymbol{\mu}}\|_2} \right\|_2 \rightarrow 0, \quad \forall c. \quad (11)$$

Instead, we use class-wise cosine similarity (Equation 8) and its variation ($\mathcal{UNC3}$).

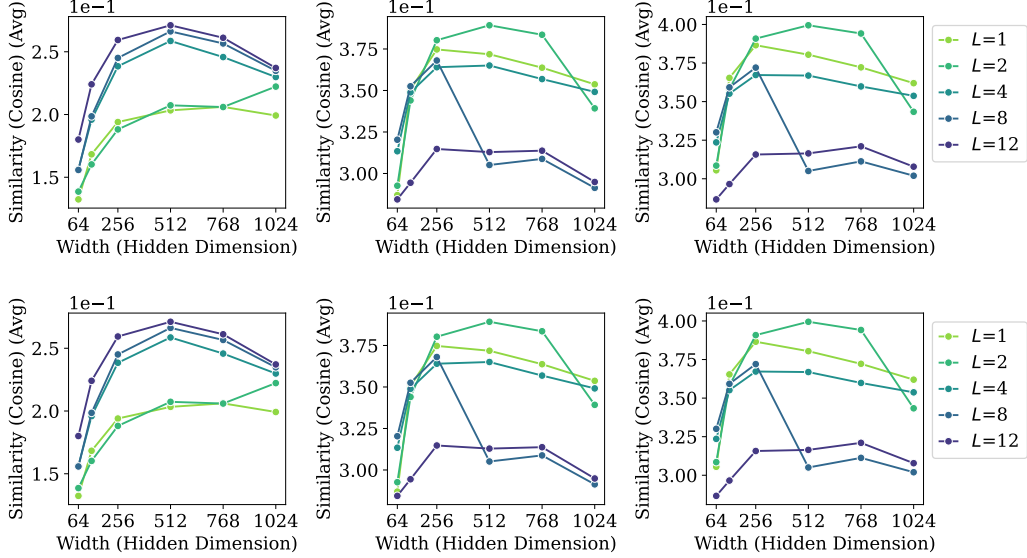


Figure 23: Average classifier alignment increases $\mathcal{NC}3$ when training for 1 (left) through 10 (right) with weight decays $\beta = 0.0005$ (top) and $\beta = 0.1$ (bottom). However, we see no meaningful trend when scaling width d , suggesting that $\mathcal{NC}3$ does not coalesce with language modelling training.

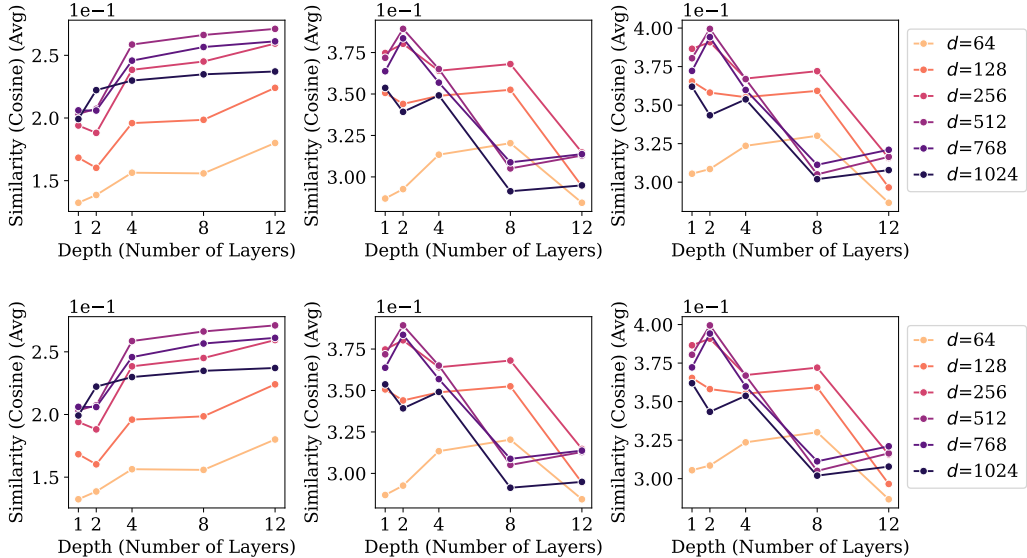


Figure 24: Average classifier alignment increases $\mathcal{NC}3$ when training for 1 (left) through 10 (right) with weight decays $\beta = 0.0005$ (top) and $\beta = 0.1$ (bottom). However, we see no meaningful trend when scaling depth L , suggesting that $\mathcal{NC}3$ does not coalesce with language modelling training.

N Uniformity Duality with Scale — \mathcal{UNC}_3

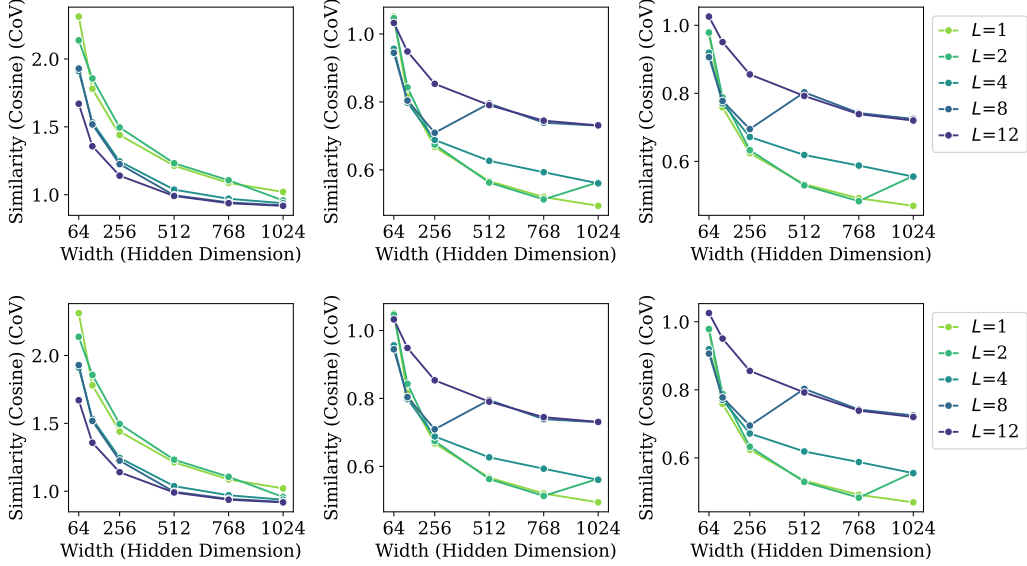


Figure 25: Variation in classifier alignment decreases when scaling width (d) in models trained for 1 (left) through 10 (right) with weight decays $\beta = 0.0005$ (top) and $\beta = 0.1$ (bottom).

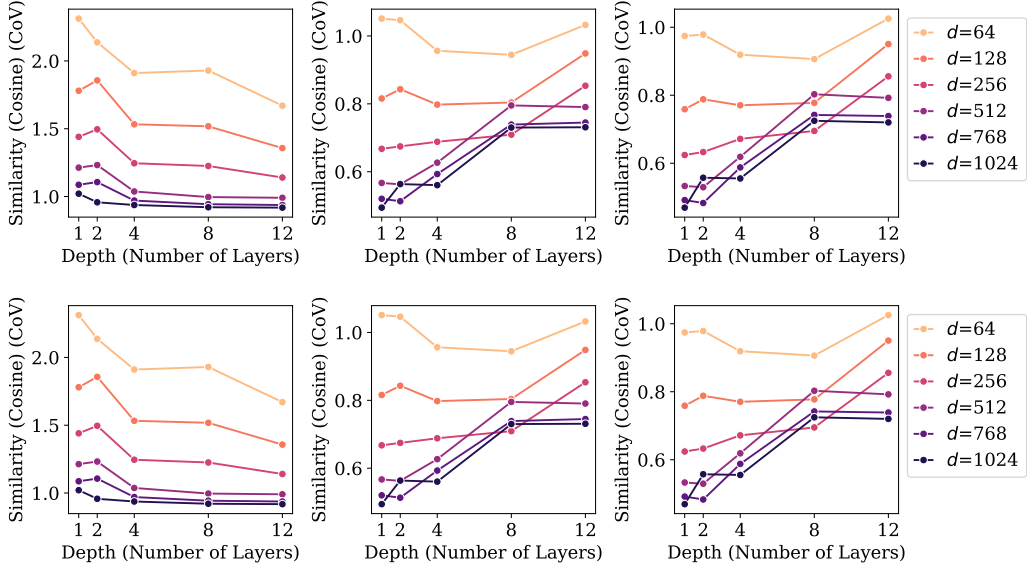


Figure 26: Variation in classifier alignment increases when scaling depth (L) in models trained for 1 (left) through 10 (right) with weight decays $\beta = 0.0005$ (top) and $\beta = 0.1$ (bottom). This negative trend of \mathcal{UNC}_3 in more learnt models (right) suggests that the link of $(\mathcal{U})\mathcal{NC}3$ with scale and performance is still weak.

O Correlations of $(\mathcal{U})\mathcal{NC}_3$ with Generalization Performance

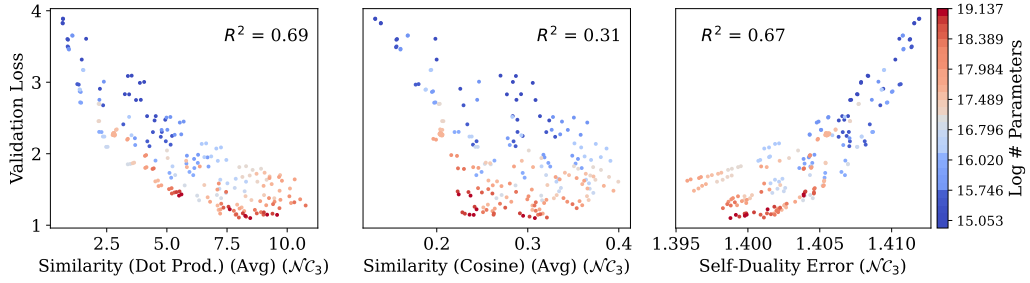


Figure 27: Generalization (validation loss) correlated with average dot-product similarity (for interpretability purposes only) (left) and cosine similarity (classifier alignment, \mathcal{NC}_3) (centre). We also computed the empirical measure from [5] (right).

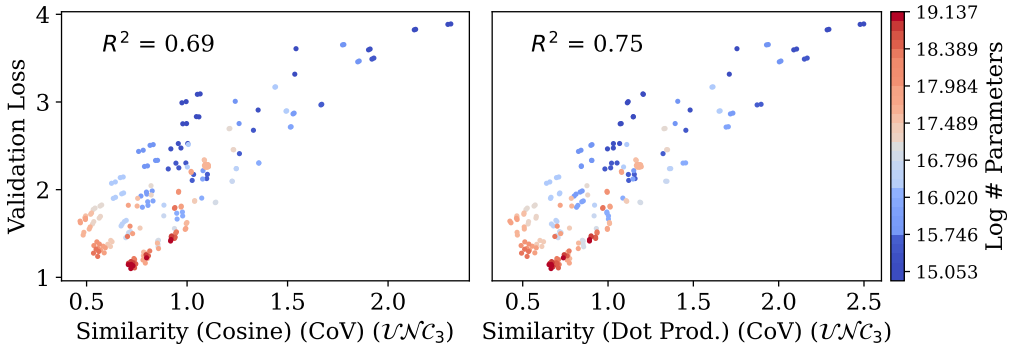


Figure 28: Generalization (validation loss) correlated with variation in dot-product similarity (for interpretability purposes only) (left) and cosine similarity (uniform duality, \mathcal{UNC}_3) (right).

P Classifier Agreement — \mathcal{NC}_4

For computational reasons, we compute Equations 9, 10 using a simple decomposition:

$$\operatorname{argmin}_{c \in \mathbb{V}} \|\mathbf{h}_b - \boldsymbol{\mu}_c\|_2 = \operatorname{argmin}_{c \in \mathbb{V}} \left(\|\mathbf{h}_b\|^2 + \|\boldsymbol{\mu}_c\|^2 - 2\mathbf{h}_b^\top \boldsymbol{\mu}_c \right) \quad (12)$$

where $b \in [1, B]$ and $c \in \mathbb{V}$ with batch size B and vocabulary \mathbb{V} .

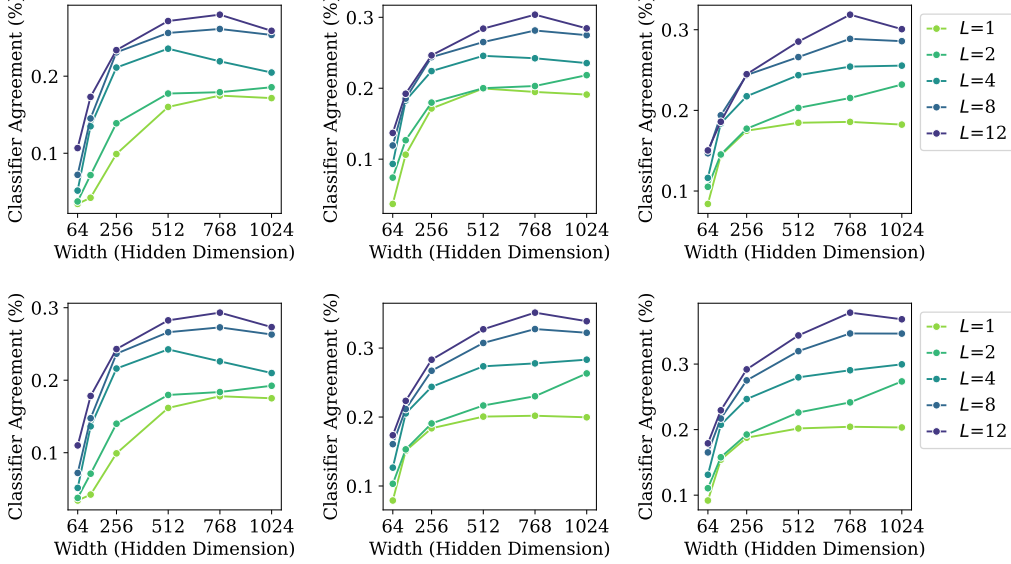


Figure 29: Classifier agreement improves when scaling width (d) in models trained for 1 (left) through 10 (right) with weight decays $\beta = 0.0005$ (top) and $\beta = 0.1$ (bottom).

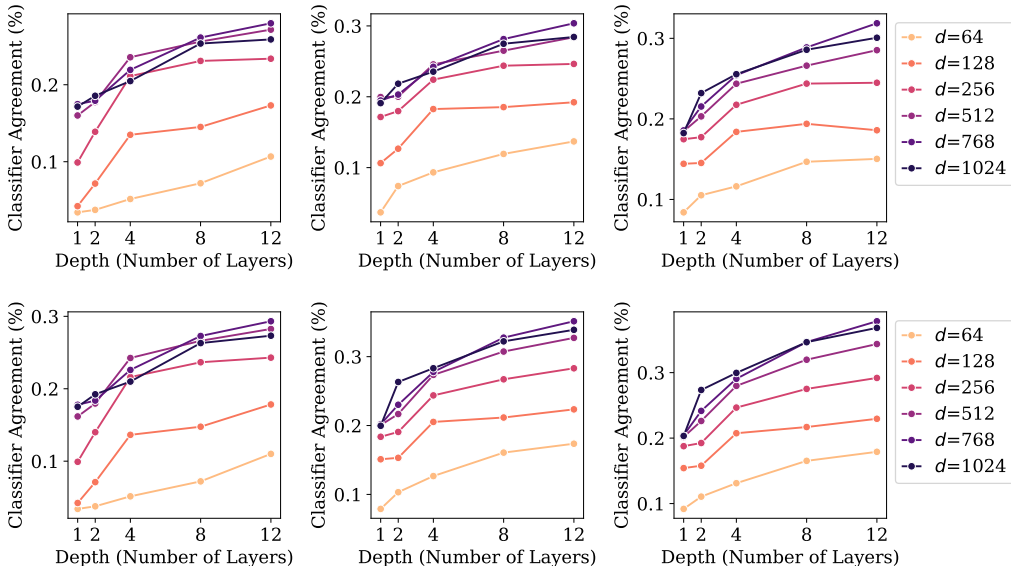


Figure 30: Classifier agreement improves when scaling depth (L) in models trained for 1 (left) through 10 (right) with weight decays $\beta = 0.0005$ (top) and $\beta = 0.1$ (bottom).

Q Examples for Interpretability

This section presents token-wise interpretability results from top-layer embeddings from our most learned model (https://huggingface.co/rhubarbwu/TinyStories-12x1024_10L).

Table 4: Under TinyStories-12x1024_10L, these fifteen homonyms have much shorter mean embedding norms (i.e. closer to the global centre) than the average token. This is expected since homonyms typically present conflicts and interference.

GPT-Neo Token ID	Token Text	Scaled Norm (Eq. 5)
808	“row”	102.9727
1806	“ring”	63.4789
2971	“light”	74.4070
4053	“well”	55.3457
4475	“date”	111.7086
8664	“bat”	83.0259
9464	“left”	81.7467
15699	“match”	114.7236
16469	“spring”	80.0322
17796	“bank”	90.8248
19204	“wave”	43.5028
19836	“close”	60.6004
22043	“fair”	57.2620
28230	“lead”	102.0583
36859	“bowl”	88.7034
(avg)	(avg)	106.8762

Table 5: Under `TinyStories-12x1024_10L`, the variability and interference of some English first names were far below those of the average token. This might be because names are distinct from one another and are not typically used in the same contexts as other words (aside from articles). The only names to have CDNV close to that of the average token are “Anna” and “Tim”. Note that the positive interference of the last row (average token) is not a typo.

GPT-Neo Token ID	Token Text	CDNV (Eq. 4)	Interference (Eq. 6)
7371	Donald	0.0000817614	-0.008308
7554	John	0.0001080000	-0.007270
11006	David	0.0000924941	-0.006167
12041	Paul	0.0000966165	-0.006768
13256	Michael	0.0000885749	-0.006625
14731	James	0.0001010000	-0.006610
14967	Tim	0.0001640000	-0.004741
17121	William	0.0000933207	-0.005867
18050	Jim	0.0001090000	-0.006896
18308	Harry	0.0001100000	-0.006749
19156	Robert	0.0000813332	-0.006438
19206	Steve	0.0000962210	-0.006541
19962	Daniel	0.0001140000	-0.006963
20191	George	0.0001080000	-0.006674
20508	Andrew	0.0000928071	-0.006036
21868	Ryan	0.0000833253	-0.006594
22405	Thomas	0.0000952689	-0.006400
23865	Kevin	0.0000939218	-0.005817
24119	Mary	0.0000884645	-0.006322
24761	Brian	0.0000855408	-0.006003
24778	Martin	0.0000966354	-0.007183
25004	Eric	0.0000973125	-0.006565
25372	Matthew	0.0000810968	-0.005544
28711	Charles	0.0000787844	-0.006371
29284	Sarah	0.0000792671	-0.006366
30730	Luke	0.0001000000	-0.005830
31160	Anna	0.0001750000	-0.005005
32476	Henry	0.0001090000	-0.006685
32697	Anthony	0.0000659484	-0.006055
34831	Kelly	0.0000858015	-0.006017
40656	Robin	0.0001180000	-0.006808
42516	Kyle	0.0000815930	-0.005333
43187	Jennifer	0.0000875091	-0.006629
43568	Elizabeth	0.0000634704	-0.006462
43687	Laura	0.0000858422	-0.005922
44484	Alice	0.0000920828	-0.006416
45572	Jessica	0.0000840532	-0.005614
46751	Jacob	0.0000912490	-0.005349
AVERAGE	AVERAGE	0.0001771000	0.000519